

# AuditVotes: A Framework Towards More Deployable Certified Robustness for Graph Neural Networks

Yuni Lai\*  
The Hong Kong Polytechnic  
University  
Hong Kong, China  
yunie.lai@connect.polyu.hk

Yulin Zhu\*  
Hong Kong Chu Hai College  
Hong Kong, China  
ylzhu@chuhai.edu.hk

Yixuan Sun  
The Hong Kong Polytechnic  
University  
Hong Kong, China  
selina.sun@connect.polyu.hk

Yulun Wu  
National University of Defense  
Technology  
Hong Kong, China  
wuyulun14@nudt.edu.cn

Bin Xiao  
The Hong Kong Polytechnic  
University  
Hong Kong, China  
b.xiao@polyu.edu.hk

Gaolei Li  
Shanghai JiaoTong University  
Hong Kong, China  
gaolei\_li@sjtu.edu.cn

Jianhua Li  
The Hong Kong Polytechnic  
University  
Hong Kong, China  
lijh888@sjtu.edu.cn

Kai Zhou†  
The Hong Kong Polytechnic  
University  
Hong Kong, China  
kaizhou@polyu.edu.hk

## Abstract

Despite advancements in Graph Neural Networks (GNNs), adaptive attacks continue to challenge their robustness. Certified robustness based on randomized smoothing has emerged as a promising solution, offering provable guarantees that a model’s predictions remain stable under adversarial perturbations within a specified range. However, existing methods face a critical trade-off between accuracy and robustness, as achieving stronger robustness requires introducing greater noise into the input graph. This excessive randomization degrades data quality and disrupts prediction consistency, limiting the practical deployment of certifiably robust GNNs in real-world scenarios where both accuracy and robustness are essential. To address this challenge, we propose **AuditVotes**, the first framework to achieve both high clean accuracy and certifiably robust accuracy for GNNs. It integrates randomized smoothing with two key components, augmentation and conditional smoothing, aiming to improve data quality and prediction consistency. The augmentation, acting as a pre-processing step, de-noises the randomized graph, significantly improving data quality and clean accuracy. The conditional smoothing, serving as a post-processing step, employs a filtering function to selectively count votes, thereby filtering low-quality predictions and improving voting consistency. Extensive experimental results demonstrate that AuditVotes significantly enhances clean accuracy, certified robustness, and empirical robustness while maintaining high computational efficiency. Notably, compared to baseline randomized smoothing, AuditVotes improves clean accuracy by 437.1% and certified accuracy by 409.3% when the attacker can arbitrarily insert 20 edges on the Cora-ML datasets, representing a substantial step toward deploying certifiably robust GNNs in real-world applications.<sup>1</sup>

## 1 Introduction

Graph Neural Networks (GNNs) [15, 25, 53, 54] have emerged as a powerful tool for learning and inference on graph-structured data, finding applications in various domains such as recommendation systems [11, 56], financial fraud detection [39], and traffic analysis [9]. Despite their success, GNNs are vulnerable to adversarial attacks [46, 59], which can significantly degrade their prediction accuracy by introducing small, carefully crafted perturbations to the input data [49, 51, 67, 68]. For instance, financial crime can modify the graph structure by manipulating their transactions to escape fraudster detection [52]. This vulnerability has prompted extensive research to develop robust GNN models [4, 23, 37, 66]. However, a central challenge lies in that the robustness of developed models can be further compromised by more advanced and *adaptive* attacks [14, 40]. Consequently, the robustness uncertainty limits the usage of GNNs in safety-critical applications. One promising solution is certified robustness [35], which aims to provide *provable* guarantees that a model’s predictions will remain stable under *any* possible adversarial perturbation within a specified range.

The most representative approach to achieving certified robustness is randomized smoothing [1, 6, 27, 35, 45, 48], which transforms any *base* classifier into a *smoothed* classifier with robustness guarantees. Specifically, randomized smoothing utilizes a majority voting mechanism, where each vote is the prediction of the base classifier over a *randomized* graph, produced by adding carefully calibrated noise to the original graph. The class with the most votes is then the final prediction, resulting in a smoothed classifier that can be proven to be robust. Despite the tremendous advances in certified robustness for GNNs in recent years, several key challenges remain, hindering the practical deployment of certifiably robust GNNs.

**Accuracy-Robustness Trade-off.** Certified robustness is primarily assessed by certified accuracy, which is the proportion of predictions that are both correct (i.e., clean accuracy) and stable

\*Equal contribution

†Corresponding author

<sup>1</sup>Source code of AuditVotes: <https://anonymous.4open.science/r/AuditVotes-6AAE/>.

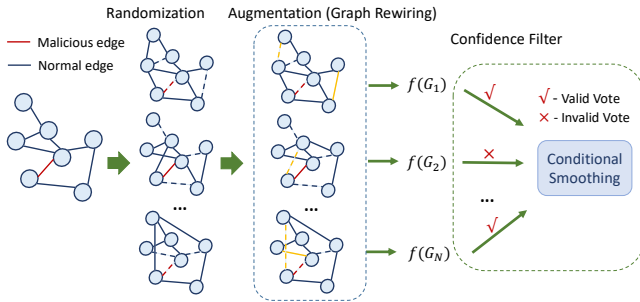


**Figure 1: AuditVotes framework introduces two added components: augmentation and conditional smoothing. The graph rewiring augmentation de-noises the randomized graph to improve data quality, and the confidence filter removes low-quality predictions to enhance prediction consistency.**

(i.e., robust ratio). Existing works [1, 20, 48, 57] have not adequately addressed this inherent trade-off: they achieve a higher robustness ratio often at a cost of introducing larger random noise to the input graph, which can severely degrade data quality and significantly diminish clean accuracy. For example, SparseSmooth [1] requires applying a higher probability of edge addition  $p_+$  to ensure a larger certified radius. However, even with a modest  $p_+$  value of 0.1, the clean accuracy of the smoothed classifier will drop to less than 0.5. Thus, a key challenge is to effectively mitigate the trade-off to make certifiably robust GNNs practically applicable.

**Prediction Consistency.** It is commonly observed that current smoothed classifiers [1, 6] often exhibit low prediction consistency, meaning that the predictions over randomized graphs vary significantly, which can lead to diminished certified performance. Consequently, several works [17–19, 33, 43] have focused on improving prediction consistency. However, these approaches often impose a heavy computational burden, resulting in significant overhead for the certification framework. Additionally, most of the proposed techniques are tailored for image classification tasks, with limited exploration in the graph learning domain. Therefore, a critical challenge is to develop efficient and graph-specific methods that enhance prediction consistency without introducing excessive computational costs.

**Robustness on unseen nodes.** For the node classification task, existing certifiably robust models focus primarily on transductive learning setting [1, 3, 20, 26, 48], where the model leveraging the complete graph during training to make predictions on known nodes (already appeared in the graph). However, as noted in [14], this transductive setting falls into a robustness pitfall: the model can remember the clean graph to achieve perfect robustness on known nodes while the robustness is unsure on unseen nodes. Furthermore, real-world applications often require GNN models to operate in an inductive setting [12, 36, 39, 42], where they must generalize to accommodate new nodes continuously introduced to the graph. For instance, in financial networks, as new accounts or transactions emerge, models must classify and analyze these entities without prior knowledge of their characteristics. This highlights the necessity of an inductive certification framework to avoid the pitfall of transductive learning and ensure superior robustness for unseen nodes under evasion attacks.

To address the above challenges, we propose **AuditVotes**, a general certification framework that can achieve both high clean accuracy and certifiably robust ratio for GNNs. Our general strategy is to keep a larger degree of randomization (for a higher robust ratio) and improve the quality of the graph data as well as the quality of votes (to restore model accuracy). To this end, AuditVotes (shown in Figure 1) introduces two components, augmentation and conditional smoothing, that are seamlessly integrated into the randomized smoothing pipeline. Specifically, we introduce graph rewiring augmentation to pre-process the randomized graphs, aiming to de-noise the randomized graph and enhance data quality by rewiring the edges. Then, we apply conditional smoothing to the prediction results of the base classifier, through which we aim to filter out some low-quality predictions using a confidence filter to improve the consistency of votes. Combining the pre-processing of graph data and post-processing of votes, we can significantly improve the overall certification performance. Moreover, we design and evaluate AuditVotes in inductive learning, in which the model is trained on a training graph and tested on new and unseen nodes.

Nevertheless, effectively fitting augmentation and conditional filters into the randomized smoothing pipeline has several challenges. First, both the augmentation process and the conditional filter must be highly efficient, as randomized smoothing typically requires thousands of model inferences, and the augmenter must handle a large number of randomized graphs. Second, the augmentation process should be adaptive to the type and level of noise added to the graph, ensuring the recovery of the original graph structure as accurately as possible. Third, the augmenter and conditional filter should be applicable in inductive learning, as the evasion attack on the graph usually presents in inductive learning that the model has not seen the testing nodes/graphs during training [7, 14]. Finally, the newly integrated components may compromise the previously established certificate, making it essential to establish a new theoretical robustness certificate for AuditVotes to ensure provable robustness guarantees.

In this paper, we instantiate AuditVotes with simple yet effective strategies. First, we introduced three graph augmentation methods that are efficient for randomized smoothing and well-suited to inductive learning: Jaccard similarity augmenter (JacAug), feature auto-encoder augmenter (FAEAug), and multi-head similarity augmenter (SimAug). These augmenters only rely on node features to make edge predictions, allowing them to generalize to unseen graphs or nodes. Additionally, they can be trained and pre-computed once prior to the smoothing process to avoid repeated computation during the smoothing. To implement conditional smoothing, we utilize model prediction confidence (Conf) as a filtering condition: only high-confidence predictions are employed for voting. Finally, we establish a theoretically robust certification for AuditVotes by making a non-trivial adaption from the existing certification. Last but not least, we note that there are other smoothing schemes, such as de-randomized smoothing for GNNs [55, 57] and randomized smoothing, Gaussian [6], for image classification [6, 50]. Our AuditVotes as a general framework can also be applied to other smoothing schemes with minor adaptation.

To validate our approach, we conduct extensive evaluations demonstrating that **AuditVotes significantly boosts clean accuracy, certified accuracy, and empirical robustness while**

**maintaining high efficiency and wide applicability.** For example, in defending against edge insertion attacks on the Citeseer dataset, our augmentation SimAug improves the clean accuracy from 14.7% to 70.9%, and our AuditVotes (SimAug+Conf) improves the certified accuracy from 14.7% to 72.6% (when the attack power is arbitrarily inserting 20 edges). Moreover, we evaluate AuditVotes as an empirical defense under Nettack [67] and IG-attack [51]. On the Cora-ML dataset, it achieves 96.7% empirical robustness when the attacker budget is 5 edges per target node. This comprehensive enhancement is of great importance for the practical deployment of GNNs in security-sensitive applications, as it provides higher accuracy and stronger guarantees of robustness. AuditVotes as a general framework also has a significant advantage when applied to other smoothing schemes such as GNNCert [57] and Gaussian [6]. For instance, AuditVotes (Conf) significantly improves the certified accuracy by 19.6% on the CIFAR-10 dataset. Notably, AuditVotes has a comparable runtime as vanilla smoothing, demonstrating its efficiency. To summarize, our contributions are listed as follows:

- We propose AuditVotes, incorporating augmentation and conditional smoothing, to provide high clean accuracy and high certifiably robust accuracy.
- We instantiate three efficient graph augmentation strategies (JacAug, FAEAug, SimAug) that are well-suited to inductive learning settings and adapt to varying levels of noise.
- We instantiate the conditional smoothing process using confidence scores (Conf), which significantly improves certified accuracy nearly for free in computation workload.
- AuditVotes is a model-agnostic and general framework that can be easily extended to other smoothing schemes, such as GNNCert [57] and Gaussian [6] (for image data).
- Through extensive evaluations, we demonstrate the superior performance of AuditVotes in boosting clean accuracy, certified accuracy, and empirical robustness, while also maintaining high efficiency and broad applicability.

## 2 Background and Problem Definition

In this section, we provide the necessary background by defining notations, describing the node classification task with GNNs, introducing certifying robustness frameworks applied to GNNs and image classifiers, and defining the threat model.

### 2.1 Inductive Node Classification

We represent a graph as  $\mathcal{G} = (\mathbf{V}, \mathbf{E}, \mathbf{X})$ , where  $\mathbf{V}$  and  $\mathbf{E}$  denote the set of nodes and edges, respectively, and  $\mathbf{X}$  is the node feature matrix of size  $|\mathbf{V}| \times d$ . We use  $\mathbf{A}$  to denote the adjacency matrix of the graph  $\mathcal{G}$ . Each node is associated with a label among  $\mathcal{Y} = \{1, 2, \dots, C\}$ , and the node classifier, such as a GNN, aims to predict the labels. To avoid the robustness pitfall of transductive learning as studied in [14], we consider a fully inductive graph learning that a GNN node classifier  $f: \mathbb{G} \rightarrow \mathcal{Y}$  is trained on a training graph  $\mathcal{G}_{train}$  and then the model can generalize to unseen nodes in the testing graph  $\mathcal{G}_{test}$ . Note that the validation nodes and testing nodes are strictly excluded from the training graph (see the experimental setup in Section 6 for more details).

### 2.2 Certified Robustness for GNNs

The certified robustness model for GNNs can be grouped as a randomized and de-randomized smoothing framework. The former adds random noise to the graph, while the latter partition the graph into several subgraphs. Then, the certificate is established based on ‘‘majority votes’’ over multiple inputs.

**2.2.1 Randomized Smoothing.** The mainstream approach to realize certified robustness is *randomized smoothing* with representative works [1, 20, 26, 27, 48] calibrated for GNNs. Specifically, given an input graph  $\mathcal{G}$  and *any* base classifier  $f(\cdot)$  (such as a GNN), they will add random noise to  $\mathcal{G}$ , resulting in a collection of randomized graphs denoted by  $\phi(\mathcal{G})$ , where  $\phi(\cdot)$  denotes the randomization process. Then, the base classifier  $f$  is used to make predictions over the random graphs, and the final prediction is obtained through majority voting. Equivalently, randomized smoothing can convert any base classifier into a *smoothed classifier*  $g(\cdot)$ , defined as:

$$g_v(\mathcal{G}) := \arg \max_{y \in \mathcal{Y}} p_{v,y}(\mathcal{G}) := \mathbb{P}(f_v(\phi(\mathcal{G})) = y), \quad (1)$$

where  $\mathbb{P}(f_v(\phi(\mathcal{G})) = y)$  denotes the probability of predicting a node  $v$  as class  $y$ . Then, it can be proved that the smoothed classifier  $g$  is provably robust with respect to a certain perturbation space  $\mathcal{B}$ , which defines the set of perturbations introduced by the attacker. In this paper, we take SparseSmooth [1] as an example, and certify against Graph Modification Attacks (GMA) perturbation where the attacker can add at most  $r_a$  edges and delete at most  $r_d$  edges among existing nodes. The  $\phi(\mathcal{G})$  is defined as randomly adding edges with probability  $p_+$  and removing edges with probability  $p_-$ . The smoothed model with larger  $p_-$  and  $p_+$  can certify larger  $r_a$  and  $r_d$ . However, a high level of noise hinders the accuracy of the smoothed model. In this paper, we aim to improve the trade-off between model accuracy and robustness.

**2.2.2 De-randomized Smoothing.** De-randomized smoothing [55, 57] divides the graphs into several groups with fixed randomness. For instance, GNNCert [57] partitions the edges  $\mathbf{E}$  in the graph into  $T_s$  groups  $\{\mathbf{E}_1, \mathbf{E}_2, \dots, \mathbf{E}_{T_s}\}$  via a hash function  $\mathcal{H}(\cdot)$ :

$$\mathbf{E}_i = \{\mathcal{H}(s_u \oplus s_v) \% T_s + 1 = i | (u, v) \in \mathbf{E}\}, \quad (2)$$

where  $i = 1, 2, \dots, T_s$ ,  $s_u$  denotes the ID of node  $u$ , and  $\oplus$  represents the concatenation of two strings. These edge sets then form  $T_s$  subgraphs  $\{\mathcal{G}_1, \mathcal{G}_2, \dots, \mathcal{G}_{T_s}\}$ . Then, the final prediction is also obtained by ‘‘majority vote’’ over  $T_s$  subgraphs:

$$g_v(\mathcal{G}) = \arg \max_{y \in \mathcal{Y}} N_v(y) := \sum_{i=1}^{T_s} \mathbb{I}\{f_v(\mathcal{G}_i) = y\}, \quad (3)$$

where  $f_v(\mathcal{G}_i)$  is a base classifier that take  $\mathcal{G}_i$  as input, and the subscript  $(\cdot)_v$  represented the classification results regarding a node  $v$ .  $N_v(y)$  denotes the number of counts that the base classifier votes class  $y$  to node  $v$ . Note that GNNCert [57] can also partition node features at the same time to defend against feature manipulation. Since we focus on structural attack, we set the group number of feature partition  $T_f = 1$  (Keep all the nodes).

Assuming that the attacker can insert several nodes to perturb the graph classification, one malicious node only shows in one subgraph. Consequently, the model is certifiably robust to a certain number of edge perturbations (addition or deletion). The group

number  $T_s$  (analogous to  $p_-$ ) controls the trade-off between model accuracy and robustness. As the  $T_s$  increases, the subgraph becomes sparser while the model can tolerate more edge perturbation. Nevertheless, the model accuracy is not satisfying because the subgraph contains poor information for each node. Hence, the accuracy-robustness trade-off also exists.

### 2.3 Certified Robustness for Image Classification

Our AuditVotes can also be generalized to improve randomized smoothing for image classification tasks [6]. Assume that  $f(\cdot)$  is a image classifier the predicts label among  $\mathcal{Y} = \{1, 2, \dots, C\}$ . The Gaussian distribution  $\epsilon \sim \mathcal{N}(0, \sigma^2 I)$  is added to the input image, and then the smoothed model  $g(\cdot)$  can be obtained by [6]:

$$g(x) = \arg \max_{y \in \mathcal{Y}} \mathbb{P}(f(x + \epsilon) = y). \quad (4)$$

It was proved that the smoothed model is certifiably robust within  $l_2$ -norm perturbation  $\{x' : \|x' - x\|_2 \leq R\}$  with radius  $R = \frac{\sigma}{2}(\Phi^{-1}(\underline{p}_A) - \Phi^{-1}(\overline{p}_B))$ , where  $\Phi^{-1}$  is the inverse of Gaussian Cumulative distribution function,  $\underline{p}_A$  is the lower bound of the top-class probability, and  $\overline{p}_B$  is the upper bound of the runner-up class probability. In this paper, we show that our proposed scheme can also be used in image classification, which is the most common domain in machine learning.

### 2.4 Threat Model

**2.4.1 Attacker.** It is known that GNN models are vulnerable to adversarial attacks [46] where the attacker can modify the input graph  $\mathcal{G}$  (e.g., structure attack) to mislead node classification. In this paper, we focus on Graph Modification Attacks (GMA) in which the attacker can modify some of the edges among the existing nodes. Specifically, we define the attacker setting as follows:

- **Attacker’s knowledge:** We assume the white-box (worst-case) attacker knows all the graph structure, node features, and node classifier.
- **Attacker’s power:** The attacker can add at most  $r_a$  edges and delete at most  $r_d$  edges among existing nodes, which we formally describe the perturbation space as:  $B_{r_a, r_d}(\mathcal{G}) := \{\mathcal{G}' \mid \sum_{ij} \mathbb{I}(A'_{ij} = A_{ij} - 1) \leq r_d, \sum_{ij} \mathbb{I}(A'_{ij} = A_{ij} + 1) \leq r_a\}$ .
- **Attacker’s goal:** The attacker aims to perturb the classification result of a target node in the testing phase (after the model training).

**2.4.2 Defender.** For any node classifier, the defender’s goal is to provide certified robustness that verifies whether the prediction for a node is consistent under a bounded attack power  $B_{r_a, r_d}(\mathcal{G})$ . Furthermore, an ideal provable defense is supposed to provide:

- **High clean accuracy:** the model accuracy on the clean graph without considering perturbation.
- **High certified accuracy:** the ratio of nodes that are both correctly classified and certifiably robust.

## 3 The AuditVotes Framework

We design AuditVotes as a general framework (Figure 1) to improve the performance of certified robustness for GNNs. The term AuditVotes derives from its two essential components, **Augmentation** and **Conditional Smoothing**, encapsulating our main idea of auditing or enhancing the quality of votes to bolster the majority-vote-based certification. Here, we introduce the high-level idea of AuditVotes and instantiate it in Section 4.

### 3.1 Noise-adaptive Augmentation

Randomized smoothing will inject undesirable noise into the graph, which is the fundamental cause of the trade-off between clean accuracy and certified robustness. Existing works often struggle to balance this trade-off effectively: achieving high certified robustness frequently results in a significant sacrifice in clean accuracy. For example, existing research shows that most attacks on GNNs prefer adding edges than deleting edges [22, 34, 46, 51, 68]. Consequently, achieving high certified accuracy against *edge addition* is practically significant. To achieve this, employing a larger  $p_+$  (i.e., probability of adding edges in randomization) becomes essential to ensure a larger certification radius. However, even with a modest  $p_+$  value of 0.1, the clean accuracy of the smoothed classifier will drop to less than 0.50 [1].

To better balance the trade-off, we propose an augmentation component that operates on the randomized graph  $\phi(\mathcal{G})$  before it goes through the base classifier  $f$ , thus serving as a *pre-processing* step to remove the noise. Our strategy is to *keep good randomization parameters* that will lead to superior certification performance, and process the randomized graph to *restore model accuracy*. Our choice for processing the randomized graphs is *graph rewiring augmentation* [8, 63], which is a widely used technique for improving the utility of input graphs by rewiring the edges.

However, effectively fitting augmentation into the randomized smoothing pipeline has several requirements. **First**, the augmentation process should be efficient, as it needs to process a large number of randomized graphs. **Second**, the augmentation should be adaptive to the specific randomization scheme, more specifically, the type and level of noise added to the graph. For instance, when the add-edge probability  $p_+$  is high, the augmentation is supposed to remove more edges in order to recover the original graph. Similarly, when  $p_-$  is high, more edges should be added. **Third**, the augmenter should be applicable in inductive learning, as the evasion attack on the graph presents in inductive learning that the model has not seen the testing nodes/graphs.

To apply augmentation, we create a function composition  $f(\mathcal{A}(\cdot))$  to be the new base classifier, where  $\mathcal{A}(\cdot)$  denotes an augmentation model. With this scheme, the existing black-box certificates such as [1, 20, 48, 57] can be easily applied to our augmented model without change because these certificates are model-agnostic. Notably, it also offers us the freedom to design the augmenter  $\mathcal{A}$ . **In Section 4, we realized three simple yet effective augmentation schemes based on node feature similarities to demonstrate the feasibility of this idea.**

### 3.2 Conditional Smoothing

While augmentation enhances the input graph, the base classifier could still make low-quality predictions over the processed graph. Robustness certificates based on randomized smoothing [1, 3, 20, 48] fundamentally depend on prediction consistency, with higher consistency leading to stronger robustness guarantees [17, 19]. To address this, we further propose a *conditional smoothing* framework that *post-process* post-processes the predictions of the base classifier before entering the voting procedure. This framework filters out low-quality predictions to enhance prediction consistency. Specifically, we define a *filtering function*, denoted as  $h(\cdot)$ , which outputs either 0 or 1, where 0 indicates that the prediction is included in the voting process and 1 excludes it. Then, we can construct a **conditional smoothed classifier**  $g^c(\cdot)$  as follows:

$$g^c(\mathcal{G}) := \arg \max_{y \in \mathcal{Y}} p_{v,y}(\mathcal{G}) := \mathbb{P}(f(\phi(\mathcal{G})) = y | h(\phi(\mathcal{G})) = 0), \quad (5)$$

where  $p_{v,y}(\mathcal{G})$  represents the probability of predicting an input graph  $\mathcal{G}$  as class  $y$  *conditioned on the criterion that*  $h(\phi(\mathcal{G})) = 0$ .

Next, we establish the conditions under which the conditional smoothed classifier is certifiably robust, which is a non-trivial adaptation from the existing certification method [1]. It is challenging that the filtering function (e.g., model prediction confidence introduced in Section 4.2) might be non-traceable, and it is not sure what kinds of random graphs are to be filtered. Nevertheless, we establish the theoretical guarantee that is suitable for arbitrarily filtering functions  $h$ . Specifically, given a node  $v$ , let  $y_A$  and  $y_B$  denote the top predicted class and the runner-up class, respectively. Let  $\underline{p}_A$  and  $\overline{p}_B$  denote the lower bound of  $p_{v,y_A}$  and the upper bound of  $p_{v,y_B}$ , respectively. We have the certificate as follows:

**THEOREM 1.** *Let the conditional smoothed classifier  $g^c(\cdot)$  be as defined in Eq. (5). We divide  $\mathbb{G}$  into  $I$  disjoint regions  $\mathbb{G} = \bigcup_{i=1}^I \mathcal{R}_i$ , where  $\mathcal{R}_i$  denote the consent likelihood ratio region that  $\frac{\mathbb{P}(\phi(\mathcal{G})=Z)}{\mathbb{P}(\phi(\mathcal{G}')=Z)} = c_i$  (a constant),  $\forall Z \in \mathcal{R}_i$ . Let  $r_i = \mathbb{P}(\phi(\mathcal{G}) \in \mathcal{R}_i)$ ,  $r'_i = \mathbb{P}(\phi(\mathcal{G}') \in \mathcal{R}_i)$  denote the probability that the random sample fall in the partitioned region  $\mathcal{R}_i$ . We define  $\mu_{r_a, r_b}$  as follows:*

$$\begin{aligned} \mu_{r_a, r_b} &:= \min_{\mathbf{s}, \mathbf{t}} \mathbf{s}^T \mathbf{r}' - \mathbf{t}^T \mathbf{r}', & (6) \\ \text{s.t. } & \mathbf{s}^T \mathbf{r} = \underline{p}_A, \mathbf{t}^T \mathbf{r} = \overline{p}_B, \quad \mathbf{s} \in [0, 1]^I, \mathbf{t} \in [0, 1]^I. \end{aligned}$$

Then for  $\forall \mathcal{G}' \in \mathcal{B}_{r_a, r_b}(\mathcal{G})$ , we have  $g_v(\mathcal{G}') = g_v(\mathcal{G})$ , if  $\mu_{r_a, r_b} > 0$ .

The proof of Theorem 1 is provided in Appendix A.1. Given the condition to determine certified robustness, Theorem 1 lays the theoretical foundation for integrating the filtering function  $h(\cdot)$  into the randomized smoothing framework. Notably, it offers us the freedom to design the function  $h$  to improve the quality of votes. In Section 4.2, we implement a simple yet effective filtering function based on the confidence of the prediction made by the classifier.

## 4 Instantiation

In this section, we instantiate the augmentation and conditional smoothing in AuditVotes with efficient and effective strategies. More implementation details and algorithms are in Appendix B.

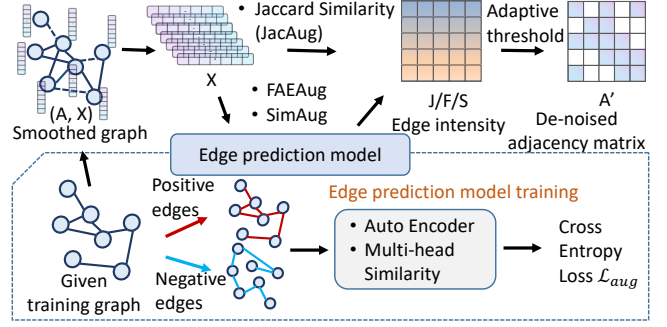


**Figure 2: We propose three graph rewiring augmentations (JacAug, FAEAUG, and SimAug). JacAug is a learning-free augmenter, and the others are learnable augmenters that are trained to recover the original graph via edge prediction.**

### 4.1 Efficient and Inductive Augmentations

We design graph rewiring augmentation (de-noise) methods that are computationally efficient, suitable for the inductive setting, and adaptive to noise levels. Randomized smoothing in the graph domain typically involves two types of noise:

- *Edge addition* (with probability  $p_+$ ), which introduces spurious edges that can increase graph density and heterophily, making it harder for the model to distinguish meaningful patterns.
- *Edge deletion* (with probability  $p_-$ ), which might remove important edges, disrupting the original graph structure and reducing connectivity.

To address the side effects introduced by the randomization, we propose three augmentation strategies—JacAug, FAEAUG, and SimAug, to de-noise the noisy graphs (Figure 2). These strategies are:

- **Efficient:** The augmentation pipeline minimizes redundant computations by precomputing reusable components (e.g., edge intensity matrix) and applying lightweight operations during inference. This design ensures scalability to large sampling sizes in randomized smoothing.
- **Adaptive:** The augmentation dynamically adjusts to noise parameters  $p_+$  and  $p_-$  by estimating the number of edge additions and deletions introduced by randomization, pruning, and recovering edges accordingly.
- **Inductive:** The augmentation methods learn transferable patterns from node features, ensuring effective generalization to unseen testing graphs.

#### 4.1.1 Augmentation based on Jaccard Similarity (JacAug).

Inspired by the simple but effective defense approach proposed for GNNs, the GCNJaccard [51], we propose a simple graph rewiring augmentation. We set a threshold  $\tau$  to prune the existing edge with  $J_{u,v} \leq \tau$ , and we add the edge if the Jaccard similarity exceeds a threshold  $\xi$ . Specifically, the Jaccard similarity (binary features) between node  $u$  and  $v$  is represented as follows:

$$J_{u,v} = \frac{\mathbf{x}_u^T \mathbf{x}_v}{\mathbf{x}_u^T \mathbf{1} + \mathbf{x}_v^T \mathbf{1} - \mathbf{x}_u^T \mathbf{x}_v}, \quad (7)$$

where the  $\mathbf{x}_u$  and  $\mathbf{x}_v$  are the node features, and  $\mathbf{1}$  denotes the all one vector, and  $T$  denotes the matrix transpose.

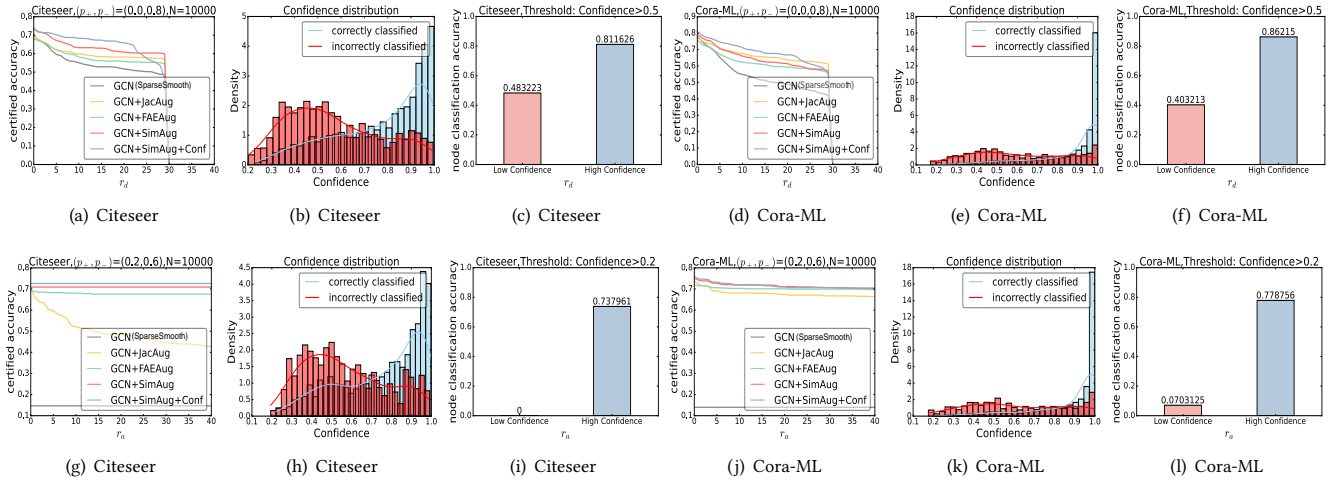


**Figure 3: Certified accuracy comparison and confidence score distribution analysis. The correctly classified nodes tend to have high confidence scores. By filtering the low-confidence predictions, conditional smoothing improves the certified accuracy.**

To reduce computation workload and avoid repeated similarity computation during smoothing, we only need to pre-calculate Jaccard similarity for all potential edges and store it in a Jaccard similarity matrix  $\mathbf{J}$ . During inference, graph rewiring is performed efficiently using the following formula:

$$\mathbf{A}' = \mathbf{A} \circ (\mathbf{J} > \tau) + (\mathbf{A} = 0) \circ (\mathbf{J} > \xi), \quad (8)$$

where  $\circ$  denotes element-wise matrix multiplication, and  $(\mathbf{J} > \tau)$  is a binary matrix where each element is 1 if  $J_{u,v} > \tau$  and 0 otherwise. The term  $\mathbf{A} \circ (\mathbf{J} > \tau)$  retains edges with  $J_{u,v} > \tau$ . Similarly,  $(\mathbf{A} = 0)$  is the complement of the adjacency matrix, where each element is 1 if  $A_{u,v} = 0$ , and the term  $(\mathbf{A} = 0) \circ (\mathbf{J} > \xi)$  adds edges with  $J_{u,v} > \xi$ .

#### 4.1.2 Augmentation based on Feature Auto-encoder (FAEAug).

Auto-encoder is widely used for graph augmentation [64]. Nevertheless, when the smoothing applies a high level of noise that randomly adds edges ( $p_+$ ), GNN-based models are ineffective because the graph becomes too dense and highly heterophilic. To tackle the challenge, we propose a simple graph augmentation that only relies on node features:

$$\mathbf{F} = \sigma(\mathbf{Z}\mathbf{Z}^T), \quad \mathbf{Z} = \mathbf{W}_1(\text{ReLU}(\mathbf{W}_2(\mathbf{X}))), \quad (9)$$

where  $\mathbf{W}_1$  and  $\mathbf{W}_2$  are trainable parameters, and  $\sigma$  is a sigmoid activation function. This augmentation model is suitable for the inductive learning setting. The parameters  $\mathbf{W}_1$  and  $\mathbf{W}_2$  trained on the training graph can be generalized to testing graphs with new nodes. Specifically, given a training subgraph, we can sample a set of positive edges  $E_{pos}$  and negative edges  $E_{neg}$ . Then, we employ binary cross-entropy loss for the graph augmentation (edge prediction) model training:

$$\begin{aligned} \mathcal{L}_{aug} = & - \frac{1}{|E_{pos} \cup E_{neg}|} \left[ \sum_{(u,v) \in E_{pos}} \log(F_{u,v}) \right. \\ & \left. + \sum_{(u,v) \in E_{neg}} \log(1 - F_{u,v}) \right], \end{aligned} \quad (10)$$

where  $F_{u,v}$  is an element in  $\mathbf{F}$  corresponding to the edge  $(u, v)$ , representing the probability of edge existence. Similarly, after the augmentation model is trained, the edge intensity matrix  $\mathbf{F}$  can also be pre-calculated once for the testing graph. The augmented adjacency matrix  $\mathbf{A}'$  is then obtained by pruning edges with  $F_{u,v} \leq \tau$  and adding edges where  $F_{u,v} > \xi$ :

$$\mathbf{A}' = \mathbf{A} \circ (\mathbf{F} > \tau) + (\mathbf{A} = 0) \circ (\mathbf{F} > \xi). \quad (11)$$

#### 4.1.3 Augmentation based on Multi-head Similarity (SimAug).

Inspired by [5, 21, 60], we implement an effective graph augmentation model based on a multi-head similarity function:

$$S_{u,v}^q = \cos(\mathbf{w}_q \circ \mathbf{x}_u, \mathbf{w}_q \circ \mathbf{x}_v), \quad S_{u,v} = \frac{1}{m} \sum_{q=1}^m S_{u,v}^q, \quad (12)$$

where  $\mathbf{w}_q$  is a trainable parameter that weighted the node feature dimension, and  $m$  is the number of heads. Compared to the Jaccard similarity, this multi-head similarity function is supposed to capture a more comprehensive pattern because different weights correspond to a different similarity function. This augmentation model is also suitable for inductive settings and follows a similar training procedure with the loss function in Eq. (10) (substituting  $F_{u,v}$  by  $S_{u,v}$ ). Once trained, the multi-head similarity matrix  $\mathbf{S}$  is pre-computed for the testing graph. The augmented adjacency matrix  $\mathbf{A}'$  is obtained by pruning edges with  $S_{u,v} \leq \tau$  and adding edges where  $S_{u,v} > \xi$ :

$$\mathbf{A}' = \mathbf{A} \circ (\mathbf{S} > \tau) + (\mathbf{A} = 0) \circ (\mathbf{S} > \xi). \quad (13)$$

**4.1.4 Noise-adaptive thresholds.** The augmentation strategies require two thresholds,  $\tau$  and  $\xi$ . We propose a simple and effective method to select noise-adaptive thresholds automatically. Specifically, given the noise parameters  $p_+$  and  $p_-$ , we can estimate the number of edges that are randomly added or deleted in the smoothing randomization. Firstly, we calculate the edge sparsity in the training graph:  $e_{ratio} := \sum \mathbf{A}_{train} / |\mathbf{V}_{train}|^2$ , where  $\mathbf{A}_{train}$  is the adjacency matrix and  $|\mathbf{V}_{train}|$  is the number of nodes in the training graph. For the testing graph, the expected number of edges before

perturbation is  $E' := e_{ratio} \times |V_{test}|^2$ . The number of edges to be added and removed is then estimated as:

$$ADD = \lfloor E' \times p_- \rfloor, \quad (14)$$

$$DEL = \lfloor (|V_{test}|^2 - E') \times p_+ \rfloor, \quad (15)$$

where  $ADD$  corresponds to edges deleted during randomization, while  $DEL$  represents spurious edges added. Threshold  $\xi$  is set based on the top- $ADD$  values (in descending order), and threshold  $\tau$  is set based on the top- $DEL$  values (in ascending order). This approach ensures that the thresholds adapt efficiently to the noise level.

## 4.2 Filtering Function

In this section, we instantiate the filtering function  $h(\cdot)$  in Eq. (5) using confidence scores predicted by the base classifier, and this technique improves the certified accuracy nearly for free in computation workload.

**4.2.1 Conditional smoothing based on confidence scores.** In this paper, we find that simply employing the prediction confidence of the base classification can effectively improve the certified accuracy. For any random sample  $\forall \mathcal{G} \in \mathbb{G}$ , the node classifier  $f$  will also return the confidence for the prediction, and we denote the confidence as  $conf(\mathcal{G})$ . Intuitively, the classifier has higher accuracy for those samples with high confidence. To explore the impact of confidence on node classification, we visualize the confidence distribution for correctly and incorrectly classified samples (Figure 3 (b,e,h,k)). Notably, the high-confidence group exhibits significantly higher node classification accuracy. Based on this observation, we use confidence as a filtering criterion. Specifically, we set a threshold  $\theta$  to filter the sample: We only keep the random sample with confidence  $conf(\phi(\mathcal{G})) > \theta$  for voting. The filtering function is defined as:

$$h(\phi(\mathcal{G})) = \begin{cases} 0 & \text{if } conf(\phi(\mathcal{G})) > \theta, \\ 1 & \text{otherwise.} \end{cases} \quad (16)$$

Note that this conditional function requires nearly no extra computation and model training.

**4.2.2 Other filtering functions.** We note that other metrics or binary classification models can also serve as the filtering function. The node homophily score [38, 65] is associated with the performance of GNNs. Furthermore, some victim node detection metrics have been proposed for graph adversarial detection, such as JSD-divergence [61]. To jointly utilize these metrics, we employ an MLP model with three combined features as its input: confidence score  $Conf(\cdot)$ , homophily score  $Homo(\cdot)$ , and JSD-divergence  $JSD(\cdot)$ . Specifically, we define  $h(\phi(\mathcal{G})) = MLP(Conf(\phi(\mathcal{G})), Homo(\phi(\mathcal{G})), JSD(\phi(\mathcal{G})))$ . Then, we can sample some noise graphs  $\phi(\mathcal{G})$  and train the MLP model on the training nodes with labels of whether they are correctly classified by the base classifier  $f$ . Nevertheless, experiments show that combining metrics provides only marginal improvements in certified accuracy (see Appendix C.1) while significantly increasing computational cost and requiring hyperparameter tuning. Thus, we recommend using confidence scores alone as a simple, effective, and computationally efficient filtering strategy.

## 5 Wide Applicability of AuditVotes

In this section, we demonstrate the wide applicability and generality of the proposed AuditVotes framework. Specifically, we show how AuditVotes can be extended to other certification schemes, including the GNN de-randomized smoothing framework GNNCert [57] and the randomized Gaussian smoothing scheme [6], originally designed for image classification.

### 5.1 Applicability for de-randomized smoothing

GNNCert [57] divides the graph's edges into several groups to create subgraphs and then uses "majority voting" based on predictions from these subgraphs to produce a robust final prediction. However, the subgraphs created by this division often have fewer edges, which can lead to reduced model accuracy.

The graph augmentation scheme in AuditVotes mitigates the loss of graph information caused by this division. Specifically, after dividing the graph into subgraphs and before classification, we apply augmentation to the subgraphs. Similar to the randomized smoothing framework, the guarantees provided by de-randomized smoothing are compatible with arbitrary base classifiers. Therefore, we can compose a new base classifier as  $f(\mathcal{A}(\cdot))$ , where  $\mathcal{A}(\cdot)$  represents graph augmentation. With this approach, the GNNCert certificate remains directly applicable to the augmented model without modification.

To implement noise-adaptive thresholds for graph augmentation in GNNCert, we exploit the absence of added edges in the subgraphs. Differently from SparseSmooth [1], GNNCert has a different type of noise. It does not involve random edge addition, but the edge division is analogous to random edge deletion with noise level controlled by the number of division groups  $T_s$ . Specifically, we set the edge-pruning threshold  $\tau = 0$  and focus on determining the edge-addition threshold  $\xi$ . Following the method in Section 4.1.4, we estimate the total number of edges in the original graph as  $E' = e_{ratio} \times |V_{test}|^2$ . Given  $T_s$  subgraph divisions, the expected number of edges to add is  $ADD = \lfloor E' \times (1 - (1/T_s)) \rfloor$ . Finally, we set the edge-addition threshold  $\xi$  based on the top- $ADD$  values.

### 5.2 Applicability for Gaussian smoothing

We extend the conditional smoothing framework of AuditVotes to Gaussian [6], the most typical and representative randomized smoothing scheme for image classification tasks. Specifically, we define the conditional smoothed model as:

$$g^c(x) = \arg \max_{y \in \mathcal{Y}} \mathbb{P}(f(x + \epsilon) = y | h(x + \epsilon) = 0), \quad (17)$$

where  $\epsilon \sim \mathcal{N}(0, \sigma^2 I)$ , and  $h(\cdot)$  is the conditional function as defined in Eq. (16). This model involves Gaussian noise in continuous space while SparseSmooth [1] employs discrete and binary noise distribution. As a result, a new certificate needs to be explored with conditional smoothing on noise continuous distribution. It is also challenging that it is not sure what kinds of random images are to be filtered. Artfully, we employ Neyman-Pearson Lemma [41] to avoid the direct estimation of  $h(\cdot)$ . Given an image  $x$ , let  $y_A$  and  $y_B$  denote the top predicted class and the runner-up class, respectively. Let  $\underline{p}_A$  and  $\overline{p}_B$  denote the lower bound of  $\mathbb{P}(f(x + \epsilon) = y_A | h(x + \epsilon) = 0)$  and the upper bound of  $\mathbb{P}(f(x + \epsilon) = y_B | h(x + \epsilon) = 0)$ , respectively.

Next, we establish the condition for the conditional smoothed classifier to be certifiably robust, which is a non-trivial adaption from the existing certification method [6].

**THEOREM 2.** *Let the conditional smoothed classifier  $g^c(\cdot)$  be as defined in Eq. (17).  $\forall x' \in \{x' : \|x' - x\|_2 \leq R\}$ , we have  $g(x') = g(x)$ , where the robust radius is defined as:*

$$R = \frac{\sigma}{2} (\Phi^{-1}(\underline{p}_A) - \Phi^{-1}(\overline{p}_B)). \quad (18)$$

The proof of Theorem 2 is provided in Appendix A.2.

## 6 Experimental Evaluations

In this section, we comprehensively evaluate our proposed certifiably robust framework AuditVotes from five aspects: clean accuracy, certified accuracy, empirical accuracy, applicability, and efficiency. In summary, we present our experimental results by answering the following research questions:

- Q1 [**Certified Accuracy**]: How effectively can AuditVotes improve certified accuracy? Why it works?
- Q2 [**Trade-off**]: How effective is AuditVotes in mitigating the trade-off between certified accuracy (robustness) and clean accuracy?
- Q3 [**Empirical Accuracy**]: How does AuditVotes perform in defending against adversarial attacks?
- Q4 [**Applicability**]: How applicable are the augmentation and conditional smoothing components to other smoothing frameworks?
- Q5 [**Efficiency**]: How efficient is AuditVotes compared to vanilla randomized smoothing and other advanced models?

### 6.1 Experimental Setup

We describe the evaluation environment, including datasets, models, baselines, parameter settings, and attack settings.

**6.1.1 Datasets.** We evaluate AuditVotes on several benchmark datasets, including graph datasets (Citeseer, Cora-ML, PubMed) and image datasets (MNIST, CIFAR-10). The statistics for these datasets are provided in Table 1 and Table 2.

**Table 1: Statistics of graph datasets.**

Datasets	Nodes	Edges	Classes	Dimension
Cora-ML	2,810	7,981	7	2,879
Citeseer	2,110	3,757	6	3,703
PubMed	19,717	44,338	3	500

For graph datasets, we adopt an inductive semi-supervised graph learning similar to [14]. Specifically, we sample 50 nodes per class for labeled training nodes ( $V_{ltrain}$ ) and validation nodes ( $V_{val}$ ). Then, in each class, we sample 20% of nodes to form testing nodes ( $V_{test}$ ) in the Citeseer and Cora-ML datasets. For the PubMed dataset, we sample 60% of nodes as testing nodes. The remaining nodes are used as unlabeled training nodes ( $V_{utrain}$ ). The training graph  $\mathcal{G}_{train}$  consists of the labeled training nodes and unlabeled training nodes ( $V_{ltrain} + V_{utrain}$ ), the validation graph involved the nodes in  $\mathcal{G}_{train}$  and validation nodes ( $V_{ltrain} + V_{utrain} + V_{val}$ ), and the testing graph  $\mathcal{G}_{test}$  involves all the nodes ( $V_{ltrain} + V_{utrain} +$

$V_{val} + V_{test}$ ). For image datasets (MNIST and CIFAR-10), we adopt the dataset configurations as detailed in Table 2.

**Table 2: Statistics of image datasets.**

Datasets	Training set	Testing set	Classes	Dimension
MNIST	60k	10k	10	$28 \times 28 \times 1$
CIFAR-10	50k	10k	10	$32 \times 32 \times 3$

#### 6.1.2 Models and Baselines.

**Node Classification Task.** For node classification, we use Spars-eSmooth [1] and GNNCert [57] as the baselines and compare with various AuditVotes configurations applied to them. The evaluated models include:

- **GCN:** The original SparseSmooth model [1] or GNNCert [57] using graph convolutional network (GCN) [25] as the base classifier.
- **GCN+JacAug:** GCN with our JacAug augmenter.
- **GCN+JacAug+Conf:** AuditVotes framework with both JacAug and the confidence filter (Conf).
- **GCN+FAEAug:** GCN with our FAEAug augmenter.
- **GCN+FAEAug+Conf:** AuditVotes framework with FAEAug and Conf.
- **GCN+SimAug:** GCN with our SimAug augmenter.
- **GCN+SimAug+Conf:** AuditVotes framework with SimAug and Conf.

Following [1], **we also evaluate APPNP [13] as the base model**, and the results are presented in Appendix C.3.

**Image Classification Task.** For the image classification task, we compare our proposed conditional smoothing to three baselines:

- 1) **Gaussian [6]:** The initial randomized smoothing model. Gaussian noise is added to the input image, and then the smoothed classification is obtained by majority voting regarding the noisy input. Noisy samples are used for augmented training samples to improve the generalization.
- 2) **Stability [33]:** It introduced a stability regularization term in the loss function to improve the prediction consistency. Specifically, the stability regularization forces the predicted probability vector of the original data and the data with Gaussian noise to be close.
- 3) **CAT-RS [18]:** It proposed a confidence-aware training strategy that uses prediction confidence to regularize the loss function. Specifically, it prevents the samples with low confidence from being highly (certified) robust while forcing high-confidence samples to be highly (certified) robust.
- 4) **Conf (Ours):** We propose a conditional smoothing framework and use confidence scores to filter the votes. Our model is a post-training process and does not need extra computation workload during training.

**Adversarial Attack Defense.** Moreover, the smoothed models can also serve as empirical robust models defending against actual adversarial attacks. We also evaluate the effectiveness of our proposed AuditVotes as an empirical robust model under Nettack [67] and IG-attack [51] (widely used structure attacks for graph data). We compare our models with regular (non-smoothed) robust GNNs:

- 1) GCN [25]: The most classical graph convolutional network.
- 2) GAT [47]: Graph attention network (GAT) employs attention layers to learn the weights for neighbor nodes during the aggregation.
- 3) MedianGCN [4]: It substitutes the weighted mean aggregation in GCN by median aggregation. The median aggregation is shown to be more robust as it is less sensitive to outliers.
- 4) AirGNN [37]: Node-wise adaptive residual was added to GNN model. It proposed an adaptive message passing that will assign more residuals on normal features that should be more consistent with local neighbors.

*Model settings and hyper-parameters.* We provide the detailed model settings and hyper-parameters in Appendix B.1.

## 6.2 Improving the Certified Accuracy (Q1)

In this section, we answer question Q1 by demonstrating the more advanced certified accuracy contributes to the AuditVotes. We evaluate its performance in defending against edge deletion perturbation (Table 3 and Figure 3 (a,d)) and edge addition perturbation (Table 4 and Figure 3 (g,j)). Specifically, we use the same smoothing parameters:  $p_+ = 0.0$ ,  $p_- = 0.8$  for certifying  $r_d$  and  $p_+ = 0.2$ ,  $p_- = 0.6$  for certifying  $r_a$ . To analyze the contribution of individual components in AuditVotes, we conduct ablation studies by applying augmentation and the confidence filter separately. Finally, we present the overall impact of the full AuditVotes framework.

**Table 3: Certified accuracy comparison ( $p_+ = 0.0$ ,  $p_- = 0.8$ ).**

datasets	model + augmentor	conditional smoothing	certified accuracy ( $r_d$ )			
			0	5	10	20
Citeseer	GCN ([1])	None	0.700	0.596	0.550	0.517
		+Conf	<b>0.748</b>	<u>0.683</u>	<u>0.656</u>	<u>0.613</u>
	GCN+JacAug	None	0.695	0.620	0.599	0.582
		+Conf	0.663	0.630	0.623	0.589
	GCN+FAEAug	None	0.680	0.620	0.582	0.558
		+Conf	0.675	0.644	0.630	0.589
	GCN+SimAug	None	<u>0.738</u>	0.671	0.632	0.608
		+Conf	0.733	<b>0.702</b>	<b>0.683</b>	<b>0.659</b>
Cora-ML	GCN ([1])	None	0.781	0.651	0.549	0.488
		+Conf	<u>0.804</u>	0.745	0.665	0.573
	GCN+JacAug	None	0.772	0.710	0.676	0.637
		+Conf	0.781	<b>0.749</b>	<b>0.735</b>	<b>0.690</b>
	GCN+FAEAug	None	0.758	0.671	0.623	0.593
		+Conf	0.770	0.726	0.687	0.653
	GCN+SimAug	None	0.793	0.704	0.660	0.614
		+Conf	<b>0.811</b>	0.745	0.712	0.667
PubMed	GCN ([1])	None	0.788	0.712	0.656	0.587
		+Conf	0.794	0.737	0.686	0.622
	GCN+JacAug	None	0.789	0.723	0.680	0.626
		+Conf	<u>0.795</u>	<u>0.746</u>	<u>0.711</u>	0.657
	GCN+FAEAug	None	0.790	0.739	0.700	0.655
		+Conf	0.789	0.745	0.709	<b>0.669</b>
	GCN+SimAug	None	<b>0.800</b>	<b>0.786</b>	<b>0.761</b>	<u>0.662</u>
		+Conf	<b>0.800</b>	<u>0.783</u>	<b>0.761</b>	<b>0.669</b>

**Table 4: Certified accuracy comparison ( $p_+ = 0.2$ ,  $p_- = 0.6$ ).**

datasets	model + augmentor	conditional smoothing	certified accuracy ( $r_a$ )			
			0	5	10	20
Citeseer	GCN ([1])	None	0.147	0.147	0.147	0.147
		+Conf	0.147	0.147	0.147	0.147
	GCN+JacAug	None	0.704	0.596	0.522	0.486
		+Conf	0.724	0.560	0.486	0.389
	GCN+FAEAug	None	0.690	0.683	0.680	0.675
		+Conf	0.697	0.690	0.688	0.685
	GCN+SimAug	None	<u>0.709</u>	<u>0.709</u>	<u>0.709</u>	<u>0.709</u>
		+Conf	<b>0.726</b>	<b>0.726</b>	<b>0.726</b>	<b>0.726</b>
Cora-ML	GCN ([1])	None	0.140	0.140	0.140	0.140
		+Conf	0.140	0.140	0.140	0.140
	GCN+JacAug	None	0.738	0.690	0.681	0.674
		+Conf	0.738	0.688	0.680	0.674
	GCN+FAEAug	None	0.719	0.706	0.703	0.701
		+Conf	0.720	0.706	0.703	0.699
	GCN+SimAug	None	<u>0.750</u>	<u>0.727</u>	<u>0.719</u>	<u>0.712</u>
		+Conf	<b>0.752</b>	<b>0.726</b>	<b>0.720</b>	<b>0.713</b>
PubMed	GCN ([1])	None	OOM	OOM	OOM	OOM
		+Conf	OOM	OOM	OOM	OOM
	GCN+JacAug	None	0.766	0.745	0.739	0.732
		+Conf	0.766	0.745	0.739	0.732
	GCN+FAEAug	None	<u>0.775</u>	<u>0.767</u>	<u>0.765</u>	<u>0.764</u>
		+Conf	<u>0.775</u>	<u>0.767</u>	<u>0.765</u>	<u>0.764</u>
	GCN+SimAug	None	<b>0.800</b>	<b>0.800</b>	<b>0.800</b>	<b>0.800</b>
		+Conf	<b>0.800</b>	<b>0.800</b>	<b>0.800</b>	<b>0.800</b>

**Table 5: Statistics of smoothed graphs ( $p_+ = 0.2$ ,  $p_- = 0.6$ ) without/with augmentation.**

datasets	graphs	reconstruction AUC	homophily
Citeseer	Original graph	1.000	0.803
	Smoothed graph	None	0.191
	+JacAug	0.899	0.821
	+FAEAug	<u>0.916</u>	<u>0.872</u>
	+SimAug	<b>0.920</b>	<b>0.895</b>
	Cora-ML	Original graph	1.000
Smoothed graph		None	0.172
+JacAug		0.817	0.792
+FAEAug		<b>0.921</b>	<u>0.866</u>
+SimAug		<u>0.836</u>	<b>0.924</b>

**6.2.1 Impact of Augmentations.** Firstly, we begin by evaluating the impact of augmentations on certified accuracy by comparing models without augmentations (GCN) and those with augmentations (JacAug, FAEAug, and SimAug). When certifying edge deletion robustness ( $r_d$ ), all three augmentations improve certified accuracy across all datasets (Table 3). For instance, in the Citeseer dataset, when the attacker deletes 20 edges ( $r_d = 20$ ), the certified accuracy improves from 51.7% (GCN) to 58.2% (GCN+JacAug), 55.8% (GCN+FAEAug), and 60.8% (GCN+SimAug). Similar improvements are observed across the Cora-ML and PubMed datasets.

Moreover, more significant improvements can be observed when certifying  $r_a$  with a high noise level of  $p_+$  (as shown in Table 4). Notably, the GCN+SimAug achieves at least 70.0% certified accuracy when  $r_a = 20$ . More specifically, SimAug improves the certified accuracy by 382.3% and 408.6% in the Citeseer and Cora-ML datasets. Note that this parameter is essential for certifying against realistic attacks that tend to add edges (Figure 11). The certified accuracy of vanilla GCN drops below 15.0% due to its low model accuracy. The noise  $p_+$  breaks the pattern of the graph, such as the homophily, and the GCN corrupts. Furthermore, the computation memory requirement increases sharply due to the graph density increasing and causes out-of-memory (OOM), especially in the PubMed dataset. In contrast, our augmentations adaptively adjust the graph’s sparsity (Figure 14), significantly mitigating these issues. As shown in Table 5, our augmentations restore the smoothed graph to the original graph with high reconstruction AUC over 0.80. Moreover, the augmentations not only recover the homophily but also enhance the homophily. These results underscore the effectiveness of our proposed augmentations in pre-processing the smoothed graphs.

**6.2.2 Impact of Confidence Filter.** Next, we investigate the impact of the conditional smoothing approach by applying the confidence filter (Conf) to GCN, GCN+JacAug, and GCN+FAEAug models. By leveraging our confidence filter, we achieve a notable enhancement in certified accuracy, especially in the case of certifying edge deletion. For all four models and in all three datasets, we observe a positive effect of the confidence filter in raising the certified accuracy (as shown in Table 3). For instance, in the Citeseer dataset, the Conf improves the certified accuracy of GCN from 51.7% to 61.3%. In Figure 4, we visualize the distribution of  $p_A$  in the vanilla smoothing (without Conf) and conditional smoothing with confidence filter (Conf). Higher  $p_A$  indicates a higher prediction consistency. We observe that the confidence filter improves the prediction consistency significantly, and this is the main reason that the Conf improves the certified accuracy.

For edge addition robustness ( $r_a$ ), the confidence filter also yields slight improvements (Table 4). This is because the prediction consistency is already high under this noise level, and it is hard to be further improved. Importantly, as shown in Section 6.6, these benefits come with minimal additional computational overhead, making the confidence filter an efficient and practical enhancement.

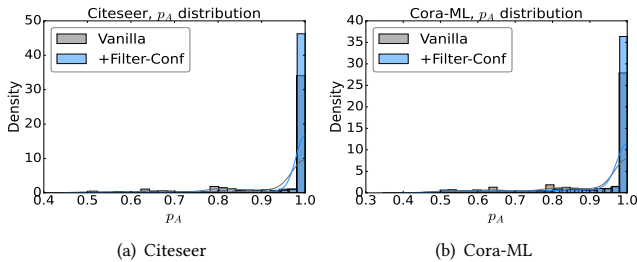


Figure 4: Prediction consistency w/o confidence filter.

**6.2.3 Overall Impact of AuditVotes.** When combining both augmentation and the confidence filter, the full AuditVotes framework achieves the most significant improvement in certified accuracy.

For edge deletion robustness ( $r_d = 20$ ), AuditVotes with SimAug and Conf achieves certified accuracy of 65.9% (Citeseer), 66.7% (Cora-ML), and 66.9% (PubMed), representing improvements of 27.5%, 36.7%, and 14.0%, respectively, compared to vanilla GCN (Table 3). Moreover, the advantage of AuditVotes is even more significant edge addition robustness (Table 4). Specifically, when  $r_a = 20$ , AuditVotes (GCN+SimAug+Conf) achieves 72.6% (Citeseer), 71.3% (Cora-ML), and 80.0% (PubMed), while the baseline GCN is not working well (with accuracy less than 15.0% or OOM errors). Compared to vanilla GCN, AuditVotes improves certified accuracy by 393.9% and 409.3% on the Citeseer and Cora-ML datasets, respectively. These results highlight the effectiveness of AuditVotes, which integrates augmentation and the confidence filter to achieve the most substantial improvements in certified accuracy.

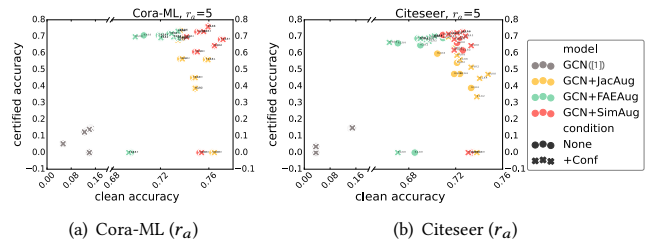


Figure 5: Clean accuracy and certified accuracy trade-off.

### 6.3 Improving the Trade-off (Q2)

Higher noise levels ( $p_+$  and  $p_-$ ) in the smoothing distribution generally result in higher certified accuracy, assuming other conditions remain constant. However, increased noise often reduces clean accuracy, thereby diminishing the model’s utility. Despite this inherent trade-off, the balance between robustness and accuracy can be significantly improved. Next, we address Q2 by demonstrating how AuditVotes effectively enhances the accuracy-robustness trade-off.

We evaluate clean accuracy and certified accuracy across various noise levels of  $p_+$  (Figure 5) and  $p_-$  (Figure 12 in Appendix). A data point indicates a better trade-off when it is closer to the upper-right corner of the plot, representing both high clean accuracy and high certified accuracy. At identical noise levels, AuditVotes consistently achieves superior clean accuracy and certified accuracy compared to the baseline.

When certifying edge addition robustness (Figure 5), the model GCN+SimAug+Conf (red cross) demonstrates the best trade-off on both the Cora-ML and Citeseer datasets. Among the other augmentations, JacAug (yellow) shows better clean accuracy in most cases, whereas FAEAug (green) achieves higher certified accuracy.

When certifying edge deletion robustness (Figure 12), the results exhibit greater diversity. Nonetheless, it is evident that all AuditVotes variants consistently outperform the baseline (vanilla smoothing with GCN, represented by gray dots). This advantage is observed across all three datasets, regardless of whether the robustness is evaluated for smaller perturbations ( $r_d = 5$ ) or larger perturbations ( $r_d = 20$ ). When verifying a larger  $r_d$  (Figure 12 (c,d,f)), we still observe that SimAug performs better than the others. These results highlight the robustness and versatility of AuditVotes in improving the trade-off between accuracy and robustness.

**Table 6: Empirical robust accuracy comparison among regular robust GNNs and smoothed GNNs. Attacker: Nettack [67] (evasion setting), with 30 targeted nodes. The attack power is the edge number the attacker can manipulate for each target node.**

datasets	defense models	regular				smoothed ( $p_+ = 0.2, p_- = 0.3, N = 1000$ )			
	attack power	GCN	GAT	MedianGCN	AirGNN	GCN (SparseSmooth)	GCN+JacAug	GCN+FAEAug	GCN+SimAug
Cora-ML	0	0.989	0.933	<b>1.000</b>	0.978	0.667	0.933	0.967	0.967
	1	0.780	0.800	0.767	0.797	0.667	0.933	<b>0.967</b>	<b>0.967</b>
	2	0.520	0.600	0.593	0.807	0.667	0.933	<b>0.967</b>	<b>0.967</b>
	3	0.393	0.480	0.427	0.747	0.667	0.933	<b>0.967</b>	<b>0.967</b>
	4	0.333	0.340	0.313	0.673	0.667	0.933	<b>0.967</b>	<b>0.967</b>
	5	0.153	0.267	0.240	0.560	0.667	0.933	<b>0.967</b>	<b>0.967</b>
Citeseer	0	0.789	0.790	0.722	0.800	0.167	0.800	0.733	<b>0.833</b>
	1	0.527	0.453	0.647	0.673	0.167	0.800	0.700	<b>0.833</b>
	2	0.240	0.273	0.340	0.527	0.167	0.767	0.700	<b>0.833</b>
	3	0.147	0.207	0.220	0.327	0.167	0.767	0.700	<b>0.833</b>
	4	0.153	0.153	0.107	0.240	0.167	0.767	0.700	<b>0.833</b>
	5	0.127	0.133	0.100	0.180	0.167	0.767	0.700	<b>0.833</b>
PubMed	0	0.793	0.800	0.767	0.760	OOM	0.833	0.833	<b>0.867</b>
	1	0.447	0.533	0.587	0.720	OOM	0.833	0.833	<b>0.867</b>
	2	0.313	0.380	0.267	0.653	OOM	0.833	0.833	<b>0.867</b>
	3	0.200	0.200	0.200	0.560	OOM	0.833	0.833	<b>0.867</b>
	4	0.167	0.153	0.167	0.447	OOM	0.833	0.833	<b>0.867</b>
	5	0.167	0.147	0.140	0.420	OOM	0.833	0.833	<b>0.867</b>

#### 6.4 More Advanced Empirical Accuracy (Q3)

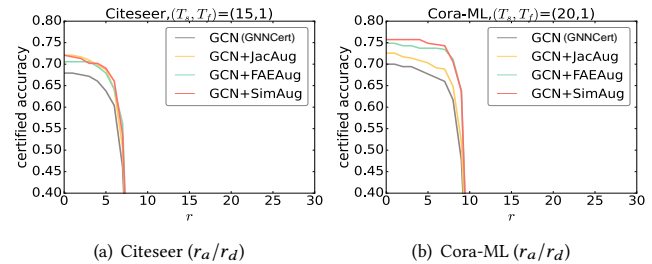
It is worth noting that randomized smoothing models can also be used as empirical defense modeling [27, 50]. In this section, we evaluate AuditVotes as a general empirical defense tool defending against actual edge modification evasion attacks. In Table 6 and Table 11 (in Appendix), we test the empirical robustness under Nettack and IG-attack with various attack power (i.e., the number of edge modification budgets per target node). The results show that AuditVotes achieves much higher robustness compared to regular robust GNN models. For example, under an attack power of 5 edges, the accuracy of AuditVotes remains nearly unchanged, whereas the accuracy of regular models declines sharply. On the Cora-ML dataset, GCN with SimAug achieves an accuracy of 96.7% while the accuracy of AirGNN is 56.0% on target nodes. Furthermore, AuditVotes maintains clean accuracy comparable to regular models across all three datasets.

Compared to the baseline GCN smoothing model, our AuditVotes smoothing maintains a high clean accuracy. In contrast, the accuracy of the baseline model is much lower, making it unable to serve as an applicable defense model. For instance, the clean accuracy of the baseline GCN smoothed model is 16.7% on Citeseer and 66.7% on Cora-ML, which are much worse than the Multilayer Perceptron (MLP) model. These results highlight the ability of AuditVotes to significantly improve both clean and empirical robust accuracy, effectively "rescuing" smoothed GNNs for practical use as robust defense models.

#### 6.5 Wide Applicability of AuditVotes (Q4)

In this section, we demonstrate the generality and wide applicability of AuditVotes. Specifically, we extend AuditVotes to other

certifying schemes, including de-randomized smoothing frameworks for GNNs [57] and randomized smoothing models for image classification tasks using Gaussian noise [6].


**Figure 6: Applying AuditVotes to GNNCert [57] on the node classification task.**
**Table 7: Certified accuracy comparison on CIFAR-10.**

$l_2$ -radius	0	0.3	0.5	0.7
Gaussian [6]	0.758	0.565	0.410	0.262
Stability [33]	0.720	0.542	0.413	0.288
CAT-RS [18]	0.711	0.627	0.564	0.489
Conf > 0.9 (Ours)	<b>0.833</b>	<b>0.752</b>	<b>0.671</b>	<b>0.535</b>

In Figure 6, we apply the augmentation component of AuditVotes to the GNNCert model to address the challenge of overly sparse graphs. Both SimAug and FAEAUG improve the clean accuracy and certified accuracy of GNNCert. For instance, on the Cora-ML dataset, SimAug increases the clean accuracy from 70.0% to

75.1% and boosts the certified accuracy (for arbitrary edge insertion/deletion with  $r$  edges) from 65.5% to 75.0%.

Furthermore, our conditional smoothing is highly applicable to randomized smoothing models in other domains. For example, we apply the confidence filter (Conf) with a threshold of 0.9 to the Gaussian [6] randomized smoothing model used for image classification tasks. As shown in Table 7, Table 10, and Figure 13 (in Appendix), Conf effectively improves certified performance. On the CIFAR-10 dataset, Conf increases clean accuracy by 9.8% and certified accuracy by 104.2% when the  $l_2$ -radius is 0.7. Similarly, on the MNIST dataset, Conf enhances certified accuracy by 4.1% at the same  $l_2$ -radius.

When compared to more advanced randomized smoothing training models, AuditVotes maintains superiority on the CIFAR-10 dataset (Figure 13(a)) and achieves comparable performance on the MNIST dataset (Figure 13(b)). Notably, Conf is computationally efficient, requiring minimal additional training time, whereas other models incur significant computational overhead. The limited improvement observed on the MNIST dataset is likely due to its already high baseline accuracy, which makes further enhancements more challenging.

## 6.6 Efficiency Comparison (Q5)

In this section, we evaluate the efficiency of AuditVotes in both node classification and image classification tasks. Table 8 presents the runtime performance when certifying edge addition perturbations (parameters:  $p_+ = 0.2$ ,  $p_- = 0.6$ ) on the Cora-ML dataset.

It is worth noting that training our augmentation requires less than 20 seconds, which is very efficient. During the testing (smoothing) phase, the edge intensity matrix, which is used for augmentation, is computed only once. Additionally, the augmentation techniques (FAEAug and SimAug) make the graph sparser, resulting in faster testing. As a result, AuditVotes models (GCN+FAEAug and GCN+SimAug) exhibit lower total runtime compared to the vanilla smoothing model (GCN).

Moreover, our conditional smoothing model (Conf) also maintains high efficiency. It uses the same training procedure as the Gaussian smoothing model, requiring no additional computations during training. In the testing phase, Conf performs  $N$  simple comparisons between confidence scores and a given threshold, introducing only a minor runtime increase. As shown in Table 8, this results in negligible additional computational cost.

In Table 9, we evaluate the runtime of various models on the CIFAR-10 dataset. The Conf model has the same training time as the Gaussian smoothing model, as it does not involve additional complexity during training. In contrast, baseline models such as Stability and CAT-RS require significantly higher training time. For example, CAT-RS requires approximately  $\times 11$  training time of the Gaussian model. During the testing (smoothing) phase, Conf only introduces less than 20 minutes of additional runtime, demonstrating its computational efficiency.

## 7 Related Works

In this section, we discuss the related existing works in certified robustness and graph data augmentation.

**Table 8: Running time comparison on Cora-ML.**

smoothed models	training	testing	total
GCN (SparseSmooth)	0:00:13	0:09:33	0:09:46
GCN+JacAug	0:00:17	0:10:11	0:10:28
GCN+FAEAug	0:00:27	0:08:51	0:09:18
GCN+SimAug	0:00:31	0:08:33	<b>0:09:04</b>
GCN+Conf	0:00:13	0:09:34	0:09:47
GCN+JacAug+Conf	0:00:17	0:10:12	0:10:29
GCN+FAEAug+Conf	0:00:27	0:08:52	<u>0:09:19</u>
GCN+SimAug+Conf	0:00:31	0:09:08	0:09:39

**Table 9: Running time comparison on CIFAR-10.**

models	training	testing	total
Gaussian [6]	00:52:59	01:59:41	<b>02:52:40</b>
Stability [33]	01:34:30	01:59:22	03:33:52
CAT-RS [18]	11:26:47	01:59:37	13:26:24
Conf (Ours)	00:52:59	02:12:24	<u>03:05:23</u>

**Certified Robustness.** The mainstream approach to realize certified robustness is *randomized smoothing* [6, 29], which is originally designed for the image classification domain. Then, it was adapted to graph domains with representative works [1, 20, 26, 27, 30, 48]. These approaches add random noise to the input, and then thousands of samples are drawn from the noise to obtain a smoothed prediction. To avoid the huge sample size and obtain a deterministic guarantee, de-randomized smoothing schemes are proposed in image domain [31, 32] and graph domain [55, 57]. In this paper, we mainly focus on the graph domain, improving both randomized and de-randomized smoothing schemes for node classification models.

The mainstream of improving certified robustness consists of de-noised smoothing and more advanced training strategies. De-noised smoothing [2, 44] employ diffusion model to de-noise the noisy input before the predictions, which can effectively improve the data quality and yield better certification performance. Nevertheless, these studies are in the image domains, and they can not be directly transferred to inductive graph learning tasks. We are the first to propose graph augmentations to de-noise the random graph.

Another way to improve certified robustness is by improving training strategies [18, 19, 33, 43, 58]. [14, 33, 43] employ adversarial training to improve the robustness of smoothed classifiers in classifying adversarial examples. [58] propose attack-free robust training that maximizes the certified radius during training, which avoids the high computation in finding adversarial examples. [19] proposed consistency regularization term to reduce the variance of predictions. Similarly, [18] design a sample-wise and confidence-aware training objective. These models, employing adversarial training, designing prediction consistency regularization, and developing adaptive noise level training, are orthogonal to our work. Compared to these approaches, our conditional smoothing based on confidence score is a *post-training* procedure that does not require extra computation during training. On the other hand, it is a general approach that can be applied to any base classifier using the training strategies above.

**Graph Data Augmentation.** Graph data augmentation [8, 63] has received lots of research efforts, and it is widely used to enhance reliable graph learning. Graph augmentation can be used as an adversarial defense technique via cleaning the perturbed graph [10, 51, 60]. For instance, GCNjaccard [51] uses the Jaccard similarity to quantify node feature similarity, removing the edges that connect dissimilar nodes to defend against add-edge adversarial attacks. Structural learning [5, 24, 64] optimizes the edge connection as a parameter with the network parameter at the same time. For example, GAUG [64] uses graph auto-encoder to implement an edge predictor to improve the performance of GNNs on node classification tasks. Despite the advancement of graph data augmentation in empirical defense, it has not been developed in the context of inductive graph learning and enhancing randomized smoothing.

## 8 Conclusion and Future Works

In this paper, we addressed critical limitations in the field of certifiably robust Graph Neural Networks (GNNs) by proposing AuditVotes, a general enhancement to the randomized smoothing framework. Our work, aiming to mitigate the trade-off between model accuracy and certified performance, is the first framework that can achieve both high model accuracy and certified accuracy for GNNs. AuditVotes incorporates two novel components: augmentation and conditional smoothing, both of which are efficient, adaptive to noise, and suitable for inductive learning scenarios.

We instantiated AuditVotes with three augmentation strategies—JacAug, FAEAug, and SimAug—that are computationally efficient and generalizable to unseen nodes. These augmenters enhance the quality of randomized graphs, leading to significant improvements in clean and certified accuracy. Additionally, we introduced conditional smoothing based on prediction confidence to exclude low-quality votes and improve voting consistency, which further boosts certified accuracy with minimal computational overhead. We establish a theoretical guarantee for the AuditVotes to obtain certified robustness. Our extensive evaluations demonstrate that AuditVotes achieves not only substantial gains in clean, certified, and empirical accuracy but also exhibits broad applicability as a general framework for enhancing other smoothing schemes, such as GNNCert and Gaussian smoothing for image classification.

By providing higher model accuracy, stronger robustness guarantees, and wide applicability, AuditVotes paves the way for the practical deployment of GNNs in security-sensitive applications where accuracy and robustness are paramount. We believe that our framework can inspire further research into exploring the more advanced designs of augmentation methods and filtering functions.

## References

- [1] Aleksandar Bojchevski, Johannes Gasteiger, and Stephan Günnemann. 2020. Efficient robustness certificates for discrete data: Sparsity-aware randomized smoothing for graphs, images and more. In *International Conference on Machine Learning*. PMLR, 1003–1013.
- [2] Nicholas Carlini, Florian Tramèr, Krishnamurthy Dvijotham, Leslie Rice, Mingjie Sun, and J Zico Kolter. 2023. (Certified!!) Adversarial Robustness for Free!. In *The Eleventh International Conference on Learning Representations*.
- [3] Jinyin Chen, Xiang Lin, Hui Xiong, Yangyang Wu, Haibin Zheng, and Qi Xuan. 2020. Smoothing adversarial training for GNN. *IEEE Transactions on Computational Social Systems* 8, 3 (2020), 618–629.
- [4] Liang Chen, Jintang Li, Qibiao Peng, Yang Liu, Zibin Zheng, and Carl Yang. 2021. Understanding structural vulnerability in graph convolutional networks. *Proceedings of the Thirtieth International Joint Conference on Artificial Intelligence* (2021).
- [5] Yu Chen, Lingfei Wu, and Mohammed Zaki. 2020. Iterative deep graph learning for graph neural networks: Better and robust node embeddings. *Advances in neural information processing systems* 33 (2020), 19314–19326.
- [6] Jeremy Cohen, Elan Rosenfeld, and Zico Kolter. 2019. Certified adversarial robustness via randomized smoothing. In *international conference on machine learning*. PMLR, 1310–1320.
- [7] Enyan Dai, Tianxiang Zhao, Huaisheng Zhu, Junjie Xu, Zhimeng Guo, Hui Liu, Jiliang Tang, and Suhang Wang. 2024. A comprehensive survey on trustworthy graph neural networks: Privacy, robustness, fairness, and explainability. *Machine Intelligence Research* (2024), 1–51.
- [8] Kaize Ding, Zhe Xu, Hanghang Tong, and Huan Liu. 2022. Data augmentation for deep graph learning: A survey. *ACM SIGKDD Explorations Newsletter* 24, 2 (2022), 61–77.
- [9] Guimin Dong, Mingyue Tang, Zhiyuan Wang, Jiechao Gao, Sikun Guo, Lihua Cai, Robert Gutierrez, Bradford Campbell, Laura E Barnes, and Mehdi Boukhechba. 2023. Graph neural networks in IoT: A survey. *ACM Transactions on Sensor Networks* 19, 2 (2023), 1–50.
- [10] Negin Entezari, Saba A Al-Sayouri, Amirali Darvishzadeh, and Evangelos E Papalexakis. 2020. All you need is low (rank) defending against adversarial attacks on graphs. In *Proceedings of the 13th international conference on web search and data mining*, 169–177.
- [11] Wenqi Fan, Yao Ma, Qing Li, Yuan He, Eric Zhao, Jiliang Tang, and Dawei Yin. 2019. Graph neural networks for social recommendation. In *The world wide web conference*, 417–426.
- [12] Xinyi Gao, Tong Chen, Yilong Zang, Wentao Zhang, Quoc Viet Hung Nguyen, Kai Zheng, and Hongzhi Yin. 2024. Graph condensation for inductive node representation learning. In *2024 IEEE 40th International Conference on Data Engineering (ICDE)*. IEEE, 3056–3069.
- [13] Johannes Gasteiger, Aleksandar Bojchevski, and Stephan Günnemann. 2019. Combining Neural Networks with Personalized PageRank for Classification on Graphs. In *International Conference on Learning Representations*.
- [14] Lukas Gosch, Simon Geisler, Daniel Sturm, Bertrand Charpentier, Daniel Zügner, and Stephan Günnemann. 2024. Adversarial training for graph neural networks: Pitfalls, solutions, and new directions. *Advances in Neural Information Processing Systems* 36 (2024).
- [15] William L. Hamilton, Rex Ying, and Jure Leskovec. 2017. Inductive representation learning on large graphs. In *Proceedings of the 31st International Conference on Neural Information Processing Systems* (Long Beach, California, USA) (NIPS’17). Curran Associates Inc., Red Hook, NY, USA, 1025–1035.
- [16] Kaiming He, Xiangyu Zhang, Shaoqing Ren, and Jian Sun. 2016. Deep residual learning for image recognition. In *Proceedings of the IEEE conference on computer vision and pattern recognition*, 770–778.
- [17] Miklós Z. Horváth, Mark Niklas Mueller, Marc Fischer, and Martin Vechev. 2022. Boosting Randomized Smoothing with Variance Reduced Classifiers. In *International Conference on Learning Representations*.
- [18] Jongheon Jeong, Seojin Kim, and Jinwoo Shin. 2023. Confidence-aware training of smoothed classifiers for certified robustness. In *Proceedings of the AAAI Conference on Artificial Intelligence*, Vol. 37, 8005–8013.
- [19] Jongheon Jeong and Jinwoo Shin. 2020. Consistency regularization for certified robustness of smoothed classifiers. *Advances in Neural Information Processing Systems* 33 (2020), 10558–10570.
- [20] Jinyuan Jia, Binghui Wang, Xiaoyu Cao, and Neil Zhenqiang Gong. 2020. Certified robustness of community detection against adversarial structural perturbation via randomized smoothing. In *Proceedings of The Web Conference 2020*, 2718–2724.
- [21] Bo Jiang, Ziyang Zhang, Doudou Lin, Jin Tang, and Bin Luo. 2019. Semi-supervised learning with graph learning-convolutional networks. In *Proceedings of the IEEE/CVF conference on computer vision and pattern recognition*, 11313–11320.
- [22] Wei Jin, Yaxing Li, Han Xu, Yiqi Wang, Shuiwang Ji, Charu Aggarwal, and Jiliang Tang. 2021. Adversarial attacks and defenses on graphs. *ACM SIGKDD Explorations Newsletter* 22, 2 (2021), 19–34.
- [23] Wei Jin, Yao Ma, Xiaorui Liu, Xianfeng Tang, Suhang Wang, and Jiliang Tang. 2020. Graph Structure Learning for Robust Graph Neural Networks. In *Proceedings of the 26th ACM SIGKDD International Conference on Knowledge Discovery & Data Mining* (Virtual Event, CA, USA) (KDD ’20). Association for Computing Machinery, New York, NY, USA, 66–74. <https://doi.org/10.1145/3394486.3403049>
- [24] Wei Jin, Yao Ma, Xiaorui Liu, Xianfeng Tang, Suhang Wang, and Jiliang Tang. 2020. Graph structure learning for robust graph neural networks. In *Proceedings of the 26th ACM SIGKDD international conference on knowledge discovery & data mining*, 66–74.
- [25] Thomas N Kipf and Max Welling. 2016. Semi-supervised classification with graph convolutional networks. *arXiv preprint arXiv:1609.02907* (2016).
- [26] Yuni Lai, PAN Bailin, Kaihuang Chen, Yancheng Yuan, and Kai Zhou. 2024. Collective Certified Robustness against Graph Injection Attacks. In *Forty-first International Conference on Machine Learning (ICML)*.

- [27] Yuni Lai, Yulin Zhu, Bailin Pan, and Kai Zhou. 2024. Node-aware Bi-smoothing: Certified Robustness against Graph Injection Attacks. In *2024 IEEE Symposium on Security and Privacy (S&P)*. IEEE Computer Society, 215–215.
- [28] Yann LeCun, Léon Bottou, Yoshua Bengio, and Patrick Haffner. 1998. Gradient-based learning applied to document recognition. *Proc. IEEE* 86, 11 (1998), 2278–2324.
- [29] Mathias Lecuyer, Vaggelis Atlidakis, Roxana Geambasu, Daniel Hsu, and Suman Jana. 2019. Certified robustness to adversarial examples with differential privacy. In *2019 IEEE symposium on security and privacy (SP)*. IEEE, 656–672.
- [30] Guang-He Lee, Yang Yuan, Shiyu Chang, and Tommi Jaakkola. 2019. Tight certificates of adversarial robustness for randomly smoothed classifiers. *Advances in Neural Information Processing Systems* 32 (2019).
- [31] Alexander Levine and Soheil Feizi. 2020. (De) Randomized smoothing for certifiable defense against patch attacks. *Advances in Neural Information Processing Systems* 33 (2020), 6465–6475.
- [32] Alexander J Levine and Soheil Feizi. 2021. Improved, deterministic smoothing for L<sub>1</sub> certified robustness. In *International Conference on Machine Learning*. PMLR, 6254–6264.
- [33] Bai Li, Changyou Chen, Wenlin Wang, and Lawrence Carin. 2019. Certified adversarial robustness with additive noise. *Advances in neural information processing systems* 32 (2019).
- [34] Kuan Li, Yang Liu, Xiang Ao, and Qing He. 2023. Revisiting graph adversarial attack and defense from a data distribution perspective. In *The Eleventh International Conference on Learning Representations*.
- [35] Linyi Li, Tao Xie, and Bo Li. 2023. Sok: Certified robustness for deep neural networks. In *2023 IEEE symposium on security and privacy (SP)*. IEEE, 1289–1310.
- [36] Shuwen Liu, Bernardo Grau, Ian Horrocks, and Egor Kostylev. 2021. Indigo: Gnn-based inductive knowledge graph completion using pair-wise encoding. *Advances in Neural Information Processing Systems* 34 (2021), 2034–2045.
- [37] Xiaorui Liu, Jiayuan Ding, Wei Jin, Han Xu, Yao Ma, Zitao Liu, and Jiliang Tang. 2021. Graph Neural Networks with Adaptive Residual. In *Thirty-Fifth Conference on Neural Information Processing Systems*.
- [38] Yao Ma, Xiaorui Liu, Neil Shah, and Jiliang Tang. 2021. Is homophily a necessity for graph neural networks? *arXiv preprint arXiv:2106.06134* (2021).
- [39] Soroor Motie and Bijan Raahemi. 2024. Financial fraud detection using graph neural networks: A systematic review. *Expert Systems with Applications* 240 (2024), 122156.
- [40] Felix Mujkanovic, Simon Geisler, Stephan Günnemann, and Aleksandar Bojchevski. 2022. Are defenses for graph neural networks robust? *Advances in Neural Information Processing Systems* 35 (2022), 8954–8968.
- [41] J. Neyman and E. S. Pearson. 1992. *On the Problem of the Most Efficient Tests of Statistical Hypotheses*. Springer New York, New York, NY, 73–108. [https://doi.org/10.1007/978-1-4612-0919-5\\_6](https://doi.org/10.1007/978-1-4612-0919-5_6)
- [42] Meng Qin, Chaorui Zhang, Bo Bai, Gong Zhang, and Dit-Yan Yeung. 2023. Towards a Better Tradeoff between quality and efficiency of community detection: An inductive embedding method across graphs. *ACM Transactions on Knowledge Discovery from Data* 17, 9 (2023), 1–34.
- [43] Hadi Salman, Jerry Li, Ilya Razenshteyn, Pengchuan Zhang, Huan Zhang, Sebastian Bubeck, and Greg Yang. 2019. Provably robust deep learning via adversarially trained smoothed classifiers. *Advances in neural information processing systems* 32 (2019).
- [44] Hadi Salman, Mingjie Sun, Greg Yang, Ashish Kapoor, and J Zico Kolter. 2020. Denoised smoothing: A provable defense for pretrained classifiers. *Advances in Neural Information Processing Systems* 33 (2020), 21945–21957.
- [45] Jan Schuchardt, Tom Wollschläger, Aleksandar Bojchevski, and Stephan Günnemann. 2023. Localized Randomized Smoothing for Collective Robustness Certification. In *The Eleventh International Conference on Learning Representations*.
- [46] Lichao Sun, Yingdong Dou, Carl Yang, Kai Zhang, Ji Wang, S Yu Philip, Lifang He, and Bo Li. 2022. Adversarial attack and defense on graph data: A survey. *IEEE Transactions on Knowledge and Data Engineering* 35, 8 (2022), 7693–7711.
- [47] Petar Veličković, Guillem Cucurull, Arantxa Casanova, Adriana Romero, Pietro Liò, and Yoshua Bengio. 2018. Graph Attention Networks. In *International Conference on Learning Representations*.
- [48] Binghui Wang, Jinyuan Jia, Xiaoyu Cao, and Neil Zhenqiang Gong. 2021. Certified robustness of graph neural networks against adversarial structural perturbation. In *Proceedings of the 27th ACM SIGKDD Conference on Knowledge Discovery & Data Mining*. 1645–1653.
- [49] Binghui Wang, Minhua Lin, Tianxiang Zhou, Pan Zhou, Ang Li, Meng Pang, Hai Li, and Yiran Chen. 2024. Efficient, direct, and restricted black-box graph evasion attacks to any-layer graph neural networks via influence function. In *Proceedings of the 17th ACM International Conference on Web Search and Data Mining*. 693–701.
- [50] Maurice Weber, Xiaojun Xu, Bojan Karlaš, Ce Zhang, and Bo Li. 2023. Rab: Provable robustness against backdoor attacks. In *2023 IEEE Symposium on Security and Privacy (SP)*. IEEE, 1311–1328.
- [51] Huijun Wu, Chen Wang, Yuriy Tyshetskiy, Andrew Docherty, Kai Lu, and Liming Zhu. 2019. Adversarial examples for graph data: deep insights into attack and defense. In *Proceedings of the 28th International Joint Conference on Artificial Intelligence*. 4816–4823.
- [52] Jiasheng Wu, Xin Liu, Dawei Cheng, Yi Ouyang, Xian Wu, and Yefeng Zheng. 2024. Safeguarding Fraud Detection from Attacks: A Robust Graph Learning Approach. In *Proceedings of the Thirty-Third International Joint Conference on Artificial Intelligence, IJCAI-24*, Vol. 8. 7500–7508.
- [53] Lingfei Wu, Peng Cui, Jian Pei, Liang Zhao, and Xiaojie Guo. 2022. Graph neural networks: foundation, frontiers and applications. In *Proceedings of the 28th ACM SIGKDD Conference on Knowledge Discovery and Data Mining*. 4840–4841.
- [54] Zonghan Wu, Shirui Pan, Fengwen Chen, Guodong Long, Chengqi Zhang, and S Yu Philip. 2020. A comprehensive survey on graph neural networks. *IEEE transactions on neural networks and learning systems* 32, 1 (2020), 4–24.
- [55] Yuxin Yang, Qiang Li, Jinyuan Jia, Yuan Hong, and Binghui Wang. 2024. Distributed backdoor attacks on federated graph learning and certified defenses. *The ACM Conference on Computer and Communications Security* (2024).
- [56] Yiwen Yuan, Zecheng Zhang, Xinwei He, Akihiro Nitta, Weihua Hu, Dong Wang, Manan Shah, Shenyang Huang, Blaž Stojanović, Alan Krumholz, et al. 2024. ContextGNN: Beyond Two-Tower Recommendation Systems. *arXiv preprint arXiv:2411.19513* (2024).
- [57] zaishuo xia, Han Yang, Binghui Wang, and Jinyuan Jia. 2024. GNNCert: Deterministic Certification of Graph Neural Networks against Adversarial Perturbations. In *The Twelfth International Conference on Learning Representations*.
- [58] Runtian Zhai, Chen Dan, Di He, Huan Zhang, Boqing Gong, Pradeep Ravikumar, Cho-Jui Hsieh, and Liwei Wang. 2020. MACER: Attack-free and Scalable Robust Training via Maximizing Certified Radius. In *International Conference on Learning Representations*.
- [59] Zhengli Zhai, Penghui Li, and Shu Feng. 2023. State of the art on adversarial attacks and defenses in graphs. *Neural Computing and Applications* (2023), 1–22.
- [60] Xiang Zhang and Marinka Zitnik. 2020. Gnguard: Defending graph neural networks against adversarial attacks. *Advances in neural information processing systems* 33 (2020), 9263–9275.
- [61] Yingxue Zhang, Florence Regol, Soumyasundar Pal, Sakif Khan, Liheng Ma, and Mark Coates. 2021. Detection and Defense of Topological Adversarial Attacks on Graphs. In *Proceedings of The 24th International Conference on Artificial Intelligence and Statistics (Proceedings of Machine Learning Research, Vol. 130)*, Arindam Banerjee and Kenji Fukumizu (Eds.). PMLR, 2989–2997.
- [62] Yingxue Zhang, Florence Regol, Soumyasundar Pal, Sakif Khan, Liheng Ma, and Mark Coates. 2021. Detection and defense of topological adversarial attacks on graphs. In *International Conference on Artificial Intelligence and Statistics*. PMLR, 2989–2997.
- [63] Tong Zhao, Wei Jin, Yozen Liu, Yingheng Wang, Gang Liu, Stephan Günnemann, Neil Shah, and Meng Jiang. 2022. Graph data augmentation for graph machine learning: A survey. *arXiv preprint arXiv:2202.08871* (2022).
- [64] Tong Zhao, Yozen Liu, Leonardo Neves, Oliver Woodford, Meng Jiang, and Neil Shah. 2021. Data augmentation for graph neural networks. In *Proceedings of the aaai conference on artificial intelligence*, Vol. 35. 11015–11023.
- [65] Jiong Zhu, Yujun Yan, Lingxiao Zhao, Mark Heimann, Leman Akoglu, and Danai Koutra. 2020. Beyond homophily in graph neural networks: Current limitations and effective designs. *Advances in neural information processing systems* 33 (2020), 7793–7804.
- [66] Yulin Zhu, Liang Tong, Gaolei Li, Xiapu Luo, and Kai Zhou. 2023. FocusedCleaner: Sanitizing Poisoned Graphs for Robust GNN-based Node Classification. *IEEE Transactions on Knowledge and Data Engineering* (2023).
- [67] Daniel Zügner, Amir Akbarnejad, and Stephan Günnemann. 2018. Adversarial attacks on neural networks for graph data. In *Proceedings of the 24th ACM SIGKDD international conference on knowledge discovery & data mining*. 2847–2856.
- [68] Daniel Zügner and Stephan Günnemann. 2019. Adversarial Attacks on Graph Neural Networks via Meta Learning. In *International Conference on Learning Representations*.

## A Proofs for Theorems

### A.1 Proof for Theorem 1

**THEOREM 1.** (Restate) Let the conditional smoothed classifier  $g^c(\cdot)$  be as defined in Eq. (5). We divide  $\mathbb{G}$  into  $I$  disjoint regions  $\mathbb{G} = \bigcup_{i=1}^I \mathcal{R}_i$ , where  $\mathcal{R}_i$  denote the consent likelihood region that satisfies  $\frac{\mathbb{P}(\phi(\mathcal{G})=Z)}{\mathbb{P}(\phi(\mathcal{G}')=Z)} = c_i$  (a constant),  $\forall Z \in \mathcal{R}_i$ . Let  $r_i = \mathbb{P}(\phi(\mathcal{G}) \in \mathcal{R}_i)$ ,  $r'_i = \mathbb{P}(\phi(\mathcal{G}') \in \mathcal{R}_i)$  denote the probability that the random sample

fall in the partitioned region  $\mathcal{R}_i$ . We define  $\mu_{r_a, r_b}$  as follows:

$$\begin{aligned} \mu_{r_a, r_b} &:= \min_{\mathbf{s}, \mathbf{t}} \mathbf{s}^T \mathbf{r}' - \mathbf{t}^T \mathbf{r}', \\ \text{s.t. } \mathbf{s}^T \mathbf{r} &= \underline{p}_A, \mathbf{t}^T \mathbf{r} = \overline{p}_B, \mathbf{s} \in [0, 1]^I, \mathbf{t} \in [0, 1]^I. \end{aligned}$$

Then for  $\forall \mathcal{G}' \in \mathcal{B}_{r_a, r_b}(\mathcal{G})$ , we have  $g_v(\mathcal{G}') = g_v(\mathcal{G})$ , if  $\mu_{r_a, r_b} > 0$ .

**PROOF.** We employ a similar proof scheme as SparseSmooth [1], and the problem of certified robustness can be formulated as a linear programming problem in (6). Specifically, given a node  $v$ , let  $y_A$  and  $y_B$  denote the top predicted class and the runner-up class, respectively. Let  $\underline{p}_A$  and  $\overline{p}_B$  denote the lower bound of  $p_{v, y_A}$  and the upper bound of  $p_{v, y_B}$ , respectively. Let  $p'_A$  and  $p'_B$  denote the probability of predicting  $y_A$  and  $y_B$  given the perturbed graph  $\mathcal{G}'$ . By the definition of the smoothed classifier  $g^c(\cdot)$  defined in Eq. (5), we know that the prediction is  $y_A$  if  $p'_A > p'_B$ . We employ the linear programming problem to find a worst-case classifier represented by vectors  $\mathbf{s}$  and  $\mathbf{t}$  such that the classification margin  $\mu_{r_a, r_b} := p'_A - p'_B$  under the perturbed graph is minimized. The vectors  $\mathbf{s} \in [0, 1]^I$  and  $\mathbf{t} \in [0, 1]^I$  encode the classifier that assigns class  $y_A$  and class  $y_B$  among the regions. More specifically,  $s_i = \mathbb{P}(f(Z) = y_A | h(Z) = 0, Z \in \mathcal{R}_i)$ , and  $t_i = \mathbb{P}(f(Z) = y_B | h(Z) = 0, Z \in \mathcal{R}_i)$ . Given that the classifier  $g^c(\cdot)$  predicts  $y_A$  for the randomized clean graph  $\phi(\mathcal{G})$  with probability at least  $\underline{p}_A$ , and predicts  $y_B$  with probability at most  $\overline{p}_B$ , the worst-case classifier satisfies  $\mathbf{s}^T \mathbf{r} = \underline{p}_A$ , and  $\mathbf{t}^T \mathbf{r} = \overline{p}_B$ . In the worst case, for  $\phi(\mathcal{G}')$ ,  $\mathbf{s}$  tends to assign the lowest probability of class  $y_A$  and  $\mathbf{t}$  tends to assign the highest probability of class  $y_B$ . Therefore, the worst-case classifier  $\mathbf{s}$  assigns class  $y_A$  in decreasing order of the constant likelihood regions until  $\mathbf{s}^T \mathbf{r} = \underline{p}_A$ , and  $\mathbf{t}$  assigns class  $y_B$  in increasing order of the constant likelihood regions until  $\mathbf{t}^T \mathbf{r} = \overline{p}_B$ . With this classifier represented by  $\mathbf{s}$  and  $\mathbf{t}$ , the classification margin  $\mu_{r_a, r_b} := p'_A - p'_B = \mathbf{s}^T \mathbf{r}' - \mathbf{t}^T \mathbf{r}'$  is minimized.

Next, we provide a simple example to further illustrate the process of decomposing the probability  $p'_A - p'_B$  into vectors  $\mathbf{s}^T \mathbf{r}' - \mathbf{t}^T \mathbf{r}'$  using the law of total probability. Assuming that there are two constant likelihood regions  $\mathcal{R}_1$  and  $\mathcal{R}_2$ , then we can decompose the conditional probabilities  $\underline{p}_A$  and  $\overline{p}_B$  as follows:

$$\begin{aligned} \underline{p}_A &= \mathbb{P}(f(\phi(\mathcal{G})) = y_A | h(\phi(\mathcal{G})) = 0) \\ &= \mathbb{P}(f(Z) = y_A | \phi(\mathcal{G}) = Z \in \mathcal{R}_1, h(Z) = 0) \\ &\quad \times \mathbb{P}(\phi(\mathcal{G}) = Z \in \mathcal{R}_1) \\ &\quad + \mathbb{P}(f(Z) = y_A | \phi(\mathcal{G}) = Z \in \mathcal{R}_2, h(Z) = 0) \\ &\quad \times \mathbb{P}(\phi(\mathcal{G}) = Z \in \mathcal{R}_2) = s_1 r_1 + s_2 r_2. \end{aligned}$$

$$\begin{aligned} \overline{p}_B &= \mathbb{P}(f(\phi(\mathcal{G})) = y_B | h(\phi(\mathcal{G})) = 0) \\ &= \mathbb{P}(f(Z) = y_B | \phi(\mathcal{G}) = Z \in \mathcal{R}_1, h(Z) = 0) \\ &\quad \times \mathbb{P}(\phi(\mathcal{G}) = Z \in \mathcal{R}_1) \\ &\quad + \mathbb{P}(f(Z) = y_B | \phi(\mathcal{G}) = Z \in \mathcal{R}_2, h(Z) = 0) \\ &\quad \times \mathbb{P}(\phi(\mathcal{G}) = Z \in \mathcal{R}_2) = t_1 r_1 + t_2 r_2. \end{aligned}$$

Next, our goal is to estimate the prediction probabilities given arbitrary perturbed graph  $\mathcal{G}' \in \mathcal{B}_{r_a, r_b}$ :

$$\begin{aligned} p'_A &:= \mathbb{P}(f(\phi(\mathcal{G}')) = y_A | h(\phi(\mathcal{G}')) = 0) \\ &= \mathbb{P}(f(Z) = y_A | \phi(\mathcal{G}') = Z \in \mathcal{R}_1, h(Z) = 0) \\ &\quad \times \mathbb{P}(\phi(\mathcal{G}') = Z \in \mathcal{R}_1) \\ &\quad + \mathbb{P}(f(Z) = y_A | \phi(\mathcal{G}') = Z \in \mathcal{R}_2, h(Z) = 0) \\ &\quad \times \mathbb{P}(\phi(\mathcal{G}') = Z \in \mathcal{R}_2) \\ &= s_1 r'_1 + s_2 r'_2. \end{aligned} \tag{19}$$

$$\begin{aligned} p'_B &:= \mathbb{P}(f(\phi(\mathcal{G}')) = y_B | h(\phi(\mathcal{G}')) = 0) \\ &= \mathbb{P}(f(Z) = y_B | \phi(\mathcal{G}') = Z \in \mathcal{R}_1, h(Z) = 0) \\ &\quad \times \mathbb{P}(\phi(\mathcal{G}') = Z \in \mathcal{R}_1) \\ &\quad + \mathbb{P}(f(Z) = y_B | \phi(\mathcal{G}') = Z \in \mathcal{R}_2, h(Z) = 0) \\ &\quad \times \mathbb{P}(\phi(\mathcal{G}') = Z \in \mathcal{R}_2) \\ &= t_1 r'_1 + t_2 r'_2. \end{aligned} \tag{20}$$

A similar decomposition can be obtained for more region numbers using the law of total probability. Finally, the prediction of sample  $\mathcal{G}$  by the smoothed classifier defined in (5) can be certified if:

$$\begin{aligned} \mu_{r_a, r_b} &= p'_A - p'_B \\ &= \mathbb{P}(f(\phi(\mathcal{G}')) = y_A | h(\phi(\mathcal{G}')) = 0) \\ &\quad - \mathbb{P}(f(\phi(\mathcal{G}')) = y_B | h(\phi(\mathcal{G}')) = 0) \\ &= \mathbf{s}^T \mathbf{r}' - \mathbf{t}^T \mathbf{r}' \\ &> 0. \end{aligned}$$

Next, the key to obtaining the certifying condition and solving the optimization problem is to find the consent likelihood  $\frac{\mathbb{P}(\phi(\mathcal{G})=Z)}{\mathbb{P}(\phi(\mathcal{G}')=Z)} = c_i$ , divide the regions  $\mathbb{G} = \bigcup_{i=1}^I \mathcal{R}_i$ , and get the probability  $r$  and  $r'$  [1, 30]. Let  $\mathcal{G}'$  denote the perturbed graph among  $\mathcal{B}_{r_a, r_b}(\mathcal{G})$ , and  $Z \in \mathbb{G}$  be any possible graph obtained by  $\phi(\mathcal{G})$  or  $\phi(\mathcal{G}')$ . We now need to compute the likelihood ratio with condition  $h(Z) = 0$ . Notably, the likelihood ratio only depends on the difference between  $\mathcal{G}$  and  $\mathcal{G}'$ , and does not depend on the filter  $h(Z)$ , so we have the likelihood ratio  $\Lambda(Z)$  as follows:

$$\Lambda(Z) = \frac{\mathbb{P}(\phi(\mathcal{G}) = Z | h(Z) = 0)}{\mathbb{P}(\phi(\mathcal{G}') = Z | h(Z) = 0)} = \frac{\mathbb{P}(\phi(\mathcal{G}) = Z)}{\mathbb{P}(\phi(\mathcal{G}') = Z)}. \tag{21}$$

That is, our conditional smoothing model (with arbitrary  $h(\cdot)$ ) does not affect the likelihood ratio, allowing us to utilize the same constant likelihood ratio region as in SparseSmooth [1]. This underscores the seamless adaptability of the certifying condition to our conditional smoothing model. The only difference lies in the definition of  $\underline{p}_A$  and  $\overline{p}_B$ . In SparseSmooth [1], the  $\underline{p}_A$  and  $\overline{p}_B$  are estimated among all the votes, while in our model, the probabilities  $\underline{p}_A$  and  $\overline{p}_B$  are estimated among the valid votes ( $h(Z) = 0$ ). Specifically, let  $X$  denote the adjacency matrix of the clean graph  $\mathcal{G}$ , and  $Y$  denote the adjacency matrix of a perturbed graph  $\mathcal{G}' \in \mathcal{B}_{r_a, r_b}(\mathcal{G})$ . We know that in the worst case, the attacker consumes all the attack budget so that  $X$  and  $Y$  have exactly  $r_a + r_d$  different bits. Let  $C = \{(k, l) | X_{kl} \neq Y_{kl}\}$  denote the location that  $X$  and  $Y$  are different, and  $X_C \in \{0, 1\}^{|C|}$  denote the elements of  $X$  in location  $C$ . We know that  $X_C$  must contain  $r_a$  zeros and  $r_d$  ones:  $\|1 - X_C\|_0 = r_a, \|X_C\|_0 = r_d$ . We can divide the space  $\mathbb{G}$  into

$r_a + r_d + 1$  disjoint regions:  $\mathbb{G} = \bigcup_{i=0}^{r_a+r_d} \mathcal{R}_i$ , where  $\mathcal{R}_i$  contains all the adjacency matrix that can be obtained by flipping  $i$  bits in  $X_C$  and have any combination of ones and zeros in the other location:

$$\mathcal{R}_i = \{Z \in \mathbb{G} : \|X_C - Z_C\|_0 = i, i = 0, 1, \dots, r_a + r_d\}. \quad (22)$$

Equivalently, the region  $\mathcal{R}_i$  contains all adjacency matrix that obtained by not flipping  $i$  bits in  $Y_C$  because  $Y_C = 1 - X_C$ . Then we have the constant likelihood:

$$\begin{aligned} \Lambda(Z)_i &= \frac{\mathbb{P}(\phi(X) = Z | h(Z) = 0)}{\mathbb{P}(\phi(Y) = Z | h(Z) = 0)} = \frac{\mathbb{P}(\phi(X) = Z)}{\mathbb{P}(\phi(Y) = Z)} \\ &= \left[ \frac{p_+}{1 - p_-} \right]^{i - r_d} \left[ \frac{p_-}{1 - p_+} \right]^{i - r_a}. \end{aligned} \quad (23)$$

Given  $r_a$  and  $r_d$ , this likelihood ratio  $\Lambda(Z)_i$  is monotonically decreasing of  $i$  if  $p_- + p_+ \leq 1$ , and monotonically decreasing, otherwise.

According to [1], the probability  $r_i = \mathbb{P}(\phi(\mathcal{G}) \in \mathcal{R}_i)$  and  $r'_i = \mathbb{P}(\phi(\mathcal{G}') \in \mathcal{R}_i)$  are Poisson-Binomial distributions:

$$r_i = \mathbb{P}(\phi(\mathcal{G}) \in \mathcal{R}_i) = PB([p_+, r_a], [p_-, r_b]), \quad (24)$$

$$r'_i = \mathbb{P}(\phi(\mathcal{G}') \in \mathcal{R}_i) = PB([1 - p_-, r_a], [1 - p_+, r_b]), \quad (25)$$

where  $PB([p_+, r_a], [p_-, r_b])$  denote Poisson-Binomial distribution with parameter  $p_+$  repeated for  $r_a$  times, and  $p_-$  repeated for  $r_d$  times:  $PB(p_+, \dots, p_+, p_-, \dots, p_-)$ . These probabilities can be calculated following the same calculation procedure as in SparseSmooth [1]. With consent likelihood  $\frac{\mathbb{P}(\phi(\mathcal{G})=Z)}{\mathbb{P}(\phi(\mathcal{G}')=Z)} = c_i$ , and the corresponding regions  $\mathcal{R}_i$ , and the probability  $r$  and  $r'$ , we can solve the optimization problem and certify the robustness.  $\square$

## A.2 Proof for Theorem 2

**THEOREM 2.** (Restate) Let the conditional smoothed classifier  $g^c(\cdot)$  be as defined in Eq. (17).  $\forall x' \in \{x' : \|x' - x\|_2 \leq R\}$ , we have  $g(x') = g(x)$ , where the robust radius is defined as:

$$R = \frac{\sigma}{2} (\Phi^{-1}(\underline{p}_A) - \Phi^{-1}(\overline{p}_B)). \quad (26)$$

**PROOF.** Given an image  $x$ , let  $y_A$  and  $y_B$  denote the top predicted class and the runner-up class, respectively. Let  $\underline{p}_A$  and  $\overline{p}_B$  denote the lower bound of  $\mathbb{P}(f(x + \epsilon) = y_A | h(x + \epsilon) = 0)$  and the upper bound of  $\mathbb{P}(f(x + \epsilon) = y_B | h(x + \epsilon) = 0)$ , respectively. We have  $g(x') = g(x)$  if  $\mathbb{P}(f(x' + \epsilon) = y_A | h(x' + \epsilon) = 0) > \max_{y_B} \mathbb{P}(f(x' + \epsilon) = y_B | h(x' + \epsilon) = 0)$ . Let's denote two random variables:

$$X := x + \epsilon = \mathcal{N}(x, \sigma^2 I),$$

$$Y := x + \delta + \epsilon = \mathcal{N}(x + \delta, \sigma^2 I),$$

where  $\delta$  satisfies:  $x + \delta = x'$ . By the definition of  $\underline{p}_A$  and  $\overline{p}_B$ , we know that:  $\mathbb{P}(f(X) = y_A | h(X) = 0) \geq \underline{p}_A$  and  $\mathbb{P}(f(X) = y_B | h(X) = 0) \leq \overline{p}_B$ . According to Neymen-Pearson Lemma adapted by Gaussian [6] (Lemma 4), we know that:

Let  $s : \mathbb{R}^d \rightarrow \{0, 1\}$  denote any function that outputs 0 or 1. If a half-space  $A = \{Z \in \mathbb{R}^d : \delta^T z \geq \beta\}$  for some  $\beta$  and  $\mathbb{P}(s(X) = 1) \leq \mathbb{P}(X \in A)$ , then  $\mathbb{P}(s(Y) = 1) \leq \mathbb{P}(Y \in A)$ . Similarly, if a half-space  $B = \{Z \in \mathbb{R}^d : \delta^T z \leq \beta\}$  for some  $\beta$  and  $\mathbb{P}(s(X) = 1) \geq \mathbb{P}(X \in A)$ , then  $\mathbb{P}(s(Y) = 1) \geq \mathbb{P}(Y \in A)$ .

We define a half-space  $A$  such that  $\mathbb{P}(X \in A) = \underline{p}_A$ , then:

$$\mathbb{P}(f(X) = y_A | h(X) = 0) \geq \underline{p}_A = \mathbb{P}(X \in A).$$

Similarly, we define a half-space  $B$  such that  $\mathbb{P}(X \in B) = \overline{p}_B$ , then:

$$\mathbb{P}(f(X) = y_B | h(X) = 0) \leq \overline{p}_B = \mathbb{P}(X \in B).$$

By applying the Neymen-Pearson Lemma above with  $s(Z) := \mathbb{1}[f(Z) = c_A] \cdot \mathbb{1}[h(Z) = 0]$  and  $s(Z) := \mathbb{1}[f(Z) = c_B] \cdot \mathbb{1}[h(Z) = 0]$ , respectively, we have:

$$\mathbb{P}(f(Y) = y_A, h(Y) = 0) \geq \mathbb{P}(Y \in A),$$

$$\mathbb{P}(f(Y) = y_B, h(Y) = 0) \leq \mathbb{P}(Y \in B).$$

Assuming that  $\mathbb{P}(h(Y) = 0) \neq 0$  (this assumption is valid because the classifier needs at least one vote for classification), by the definition of joint distribution, we have:

$$\mathbb{P}(f(Y) = y_A | h(Y) = 0) \geq \frac{\mathbb{P}(Y \in A)}{\mathbb{P}(h(Y) = 0)},$$

$$\mathbb{P}(f(Y) = y_B | h(Y) = 0) \leq \frac{\mathbb{P}(Y \in B)}{\mathbb{P}(h(Y) = 0)}.$$

Then, we have  $\mathbb{P}(f(Y) = y_A | h(Y) = 0) \geq \mathbb{P}(f(Y) = y_B | h(Y) = 0)$  if  $\mathbb{P}(Y \in A) \geq \mathbb{P}(Y \in B)$ . Next, we define the half-space following [6]:

$$A := \{Z : \delta^T (Z - x) \leq \sigma \|\delta\| \Phi^{-1}(\underline{p}_A)\},$$

$$B := \{Z : \delta^T (Z - x) \geq \sigma \|\delta\| \Phi^{-1}(1 - \overline{p}_B)\}.$$

We compute the probability that  $\mathbb{P}(Y \in A)$  and  $\mathbb{P}(Y \in B)$ :

$$\mathbb{P}(Y \in A) = \Phi(\Phi^{-1}(\underline{p}_A) - \frac{\|\delta\|}{\sigma}),$$

$$\mathbb{P}(Y \in B) = \Phi(\Phi^{-1}(\overline{p}_B) + \frac{\|\delta\|}{\sigma}).$$

Finally, we have the certifying condition that:  $g(x') = g(x)$  if  $\|\delta\|_2 < \frac{\sigma}{2} (\Phi^{-1}(\underline{p}_A) - \Phi^{-1}(\overline{p}_B))$ .  $\square$

## B More Implementation Details

### B.1 Modeling settings and hyper-parameters

For the node classifications, we employ a 2-layer GCN with the hidden layer dimension of size 128. We use learning rate  $lr = 0.001$ , regularization coefficient  $\lambda = 1 \times 10^{-3}$  for training. Early stop with patience 100 epochs and maximum 1000 epochs is employed to control the training epochs. For the CIFAR-10 dataset, we employ ResNet-110 [16] model with learning rate  $lr = 0.01$ , regularization coefficient  $\lambda = 1 \times 10^{-4}$ , batch size 256, and 150 training epochs. For the MNIST dataset, we employ LeNet [28] model with learning rate  $lr = 0.01$ , Adam optimizer, regularization coefficient  $\lambda = 1 \times 10^{-4}$ , batch size 256, and 150 training epochs. For all the randomized smoothing models, we set  $N = 10,000$  and  $\alpha = 0.001$  for Monte Carlo probability approximation in [1, 6]. In node classification, we search the noise levels among  $p_+ = \{0.0, 0.1\}$ ,  $p_- = \{0.4, 0.6, 0.7, 0.8\}$  for certifying edge deletion, and  $p_+ = \{0.2, 0.4\}$ ,  $p_- = \{0.0, 0.2, 0.4, 0.6\}$  for certifying edge addition. For GNNCert [57], we employ the MD5 hash function to divide the edges with  $T_s = 15$  for Citeseer and  $T_s = 20$  for Cora-ML because the Citeseer contains fewer edges. We set the noise level  $\sigma = 0.25$  for image classification tasks. For augmentation training, we sample 90% of existing edges in the training subgraph as the positive edges, and sample non-edges in a quantity 10 times that of the positive edges as negative edges. Then,

we train the augmentation models with a learning rate  $lr = 0.001$  using Adam optimizer for 250 epochs. In the conditional smoothing model, we set the confidence threshold as  $\theta = 0.5$  for certifying edge deletion,  $\theta = 0.2$  for certifying edge addition, and  $\theta = 0.9$  for certifying image classification. In the graph structure attacks (Nettack [67] and IG-attack [51]), we select 30 target nodes following [67] and evaluate the accuracy among these target nodes. We set the attacker budget as  $\{1, 2, 3, 4, 5\}$  edges per target node. For all the baselines, we employed the recommended parameters in their papers.

## B.2 Model Training

*Base model.* For randomized smoothing models, we follow the training setting in [1, 6, 27]. Specifically, during the training phase, we add the same random noise into the training data to improve the accuracy of the base model. For de-randomized smoothing models, we follow [57] that includes all the subgraphs induced from the training graph for training.

*Augmentation models.* For augmentation training, we sample 90% of existing edges in the training subgraph as the positive edges, and sample non-edges in a quantity 10 times that of the positive edges as negative edges. These positive and negative edges are used to train the edge prediction models in FAEAUG and SimAug with loss functions in Eq. (10). After the augmenter is trained, we apply it to the testing graph and pre-calculate the edge intensity matrix.

## B.3 Certificate Calculation

---

### Algorithm 1 AuditVotes certified robustness for node classification

---

**Require:** Clean testing graph  $\mathcal{G}$ , smoothing distribution  $\phi(G)$  with parameters  $p_+$  and  $p_-$ , trained base classifier  $f(\cdot)$ , trained augmenter  $\mathcal{A}(\cdot)$ , conditional filtering function  $h(\cdot)$ , sample size  $N$ , confidence level  $\alpha$ , perturbation budget  $r_a$  and  $r_d$ .

- 1: Draw  $N$  random graphs  $\{\mathcal{G}_i | \mathcal{G}_i \sim \phi(\mathcal{G})\}_{i=1}^N$ .
  - 2: Pre-process the random graphs with augmenter  $\mathcal{A}(\mathcal{G}_i)$ , for  $i = 1, \dots, N$ .
  - 3: Counts the votes for each class:  $counts = |\{i : f(\mathcal{A}(\mathcal{G}_i)) = y \cap h(\mathcal{A}(\mathcal{G}_i)) = 0\}|$ , for  $y = 1, \dots, C$ .
  - 4: Total valid counts:  $N_v = sum(counts)$ .
  - 5:  $y_A, y_B = \text{top two indices in } counts$ .
  - 6:  $n_A, n_B = counts[y_A], counts[y_B]$ .
  - 7:  $\underline{p}_A, \overline{p}_B = CP\_Bernolli(n_A, n_B, N_v, \alpha)$ .
  - 8: **if**  $\text{Binomial}(n_A + n_B, \frac{1}{2}) > \alpha$  **then**
  - 9:     **return** ABSTAIN
  - 10: **if**  $\mu_{r_a, r_b} > 0$  **then**
  - 11:     **return** Certified prediction  $y_A$ .
  - 12: **end if**
  - 13: **end if**
- 

*Probability lower bound.* We employ Monte Carlo probability approximation following [1, 6, 20]. Specifically, we draw  $N$  samples to estimate the Clopper-Pearson Bernoulli confidence interval with adjusted confidence  $\alpha/C$ , where  $\alpha$  is the confidence level and  $C$  is the number of classes.

*Certified accuracy.* We describe the process of obtaining certified robustness in Algorithm 1. We employ the same procedures to calculate the  $\mu_{r_a, r_b}$  as in SparseSmooth [1], and the intuition of the calculation is included in the Proof of Theorem 1 (Appendix A.1). The certified accuracy can be obtained by the ratio of nodes that are both correctly classified by the smoothed classifier (i.e.,  $y_A = y_{true}$ ), and the prediction is certified to be robust.

## C Additional Experimental Results

### C.1 Other Filtering Functions

Previous studies [65] have revealed that homophily is an important factor for node classification performance. Empirically, the graph neural networks perform better for nodes with higher homophily. However, the homophily requires the label information, which is not available during the testing. Instead, we use the pseudo label (predicted by the base classifier) to calculate the node homophily. Given a node  $v$ , the node homophily  $homo(\cdot)$  is calculated as follows:

$$homo(\mathcal{G})_v = \frac{|\{u \in \mathcal{N}(v) : \hat{y}_v = \hat{y}_u\}|}{|\mathcal{N}(v)|}, \quad (27)$$

where  $\mathcal{V}$  is the set of nodes,  $\mathcal{N}(v)$  is the neighbor of node  $v$ , and  $\hat{y}_v$  is the predicted class of node  $v$ . If all the neighbors of the node  $v$  have the same (different) predicted label, then the homophily is  $homo = 1$  (0). In particular, if a node is an isolated node, we set its homophily  $homo = 0$ .

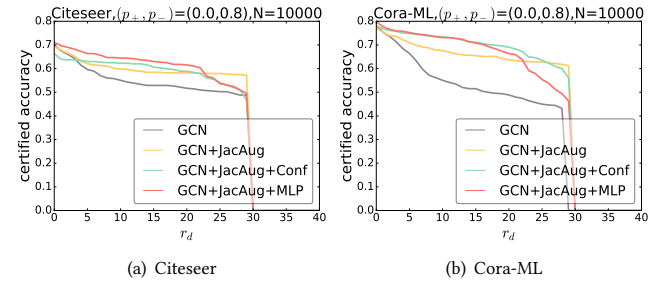


Figure 7: Other filtering function for conditional smoothing.

JSDivergence [62] measures the discrepancy of a probability vector, aiming to detect victim nodes targeted by an attacker. The intuition is that the attacker prefers adding edges between nodes with different classes, and this might enlarge the probability discrepancy between neighbors. Specifically, for a node  $v$ , the  $JSD(\cdot)$  is calculated as follows:

$$JSD(\mathcal{G})_v = H\left(\frac{1}{|\mathcal{N}(v)|} \sum_{u \in \mathcal{N}(v)} p_u\right) - \frac{1}{|\mathcal{N}(v)|} \sum_{u \in \mathcal{N}(v)} H(p_u),$$

where  $p_u$  is the softmax probability vector of node  $u$  predicted by base classifier  $f$ , and  $H(\cdot)$  denotes the Shannon entropy.

To jointly utilize these metrics, we employ an MLP model with three combined features as its input:  $h(\phi(\mathcal{G})) = MLP(Conf(\phi(\mathcal{G})), Homo(\phi(\mathcal{G})), JSD(\phi(\mathcal{G})))$ . Then, we can sample some noise graphs  $\phi(\mathcal{G})$  and train the MLP model on the training nodes with labels of whether they are correctly classified by the base classifier  $f$ . Nevertheless, we occasionally observe slight improvement when using

combined metrics (Figure 7). Compared to using confidence scores alone, it requires much more computation and hyper-parameter tuning in training the MLP model.

## C.2 Hyper-parameter Analysis

In this section, we conduct a hyper-parameter analysis regarding the threshold for the confidence filter. In Figure 8, we present the edge deletion certified accuracy of conditional smoothing with various confidence thresholds on graph datasets. In Figure 9, we present the  $l_2$ -norm certified accuracy of conditional smoothing with various confidence thresholds on the CIFAR-10 dataset. We note that in different datasets, the optimal confidence thresholds might vary. For convenience, we simply set the same confidence threshold for all datasets. In practice, this confidence threshold can be adjusted according to the performance of the validation nodes.

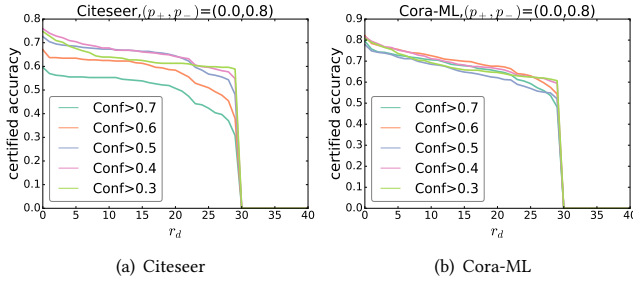


Figure 8: Certified accuracy of conditional smoothing with various confidence thresholds on graph datasets.

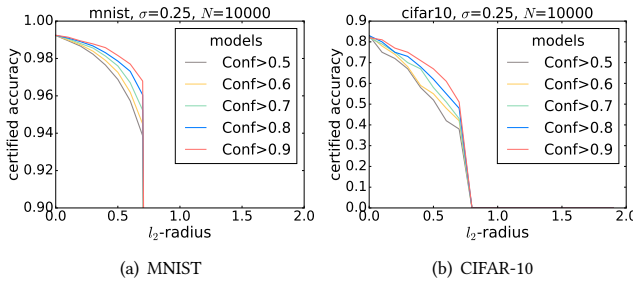


Figure 9: Certified accuracy of conditional smoothing with various confidence thresholds on image datasets.

## C.3 Other GNN base model

Following SparseSmooth [1], we also evaluate APPNP [13] as the base node classification model. In Figure 10, we present the results of the smoothed model without (APPNP) and with our augmentations (JacAug, FAEAug, and SimAug) and conditional smoothing (Conf). We observe that the APPNP+SimAug significantly outperforms the vanilla APPNP smoothing model regarding both clean accuracy and certified accuracy. When certifying edge deletion ( $r_d$ ), conditional smoothing with the confidence filter (Conf) can further improve

the performance. These results are consistent with using GCN as the base model in the main paper.

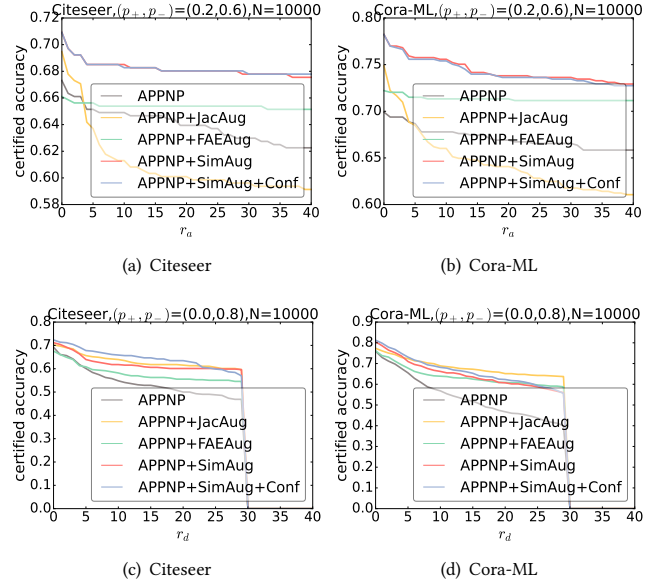


Figure 10: Using APPNP as the base GNN model for randomized smoothing.

## C.4 More other results

We put more other experimental results here due to the space limit. Specifically, we visualize the number of edges changed by Nettack and IG-attack in Figure 11. We provide the results of clean accuracy and certified accuracy trade-off for certifying edge-deletion perturbation ( $r_d$ ) in Figure 12. Empirical robustness comparison against another attack (IG-attack) is provided in Table 11. Figure 14 visualize the edge sparsity of the original graph, smoothed graph before and after augmentation. Certified accuracy evaluation on CIFAR-10 and MNIST datasets are provided in Table 13 and Table 10. Results discussion are provided in the main paper.

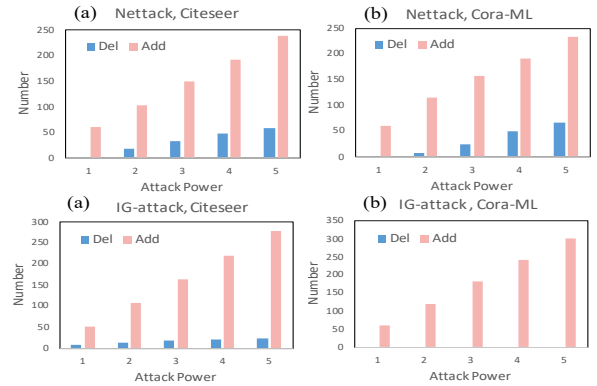


Figure 11: Attackers prefer adding edges than deleting edges.

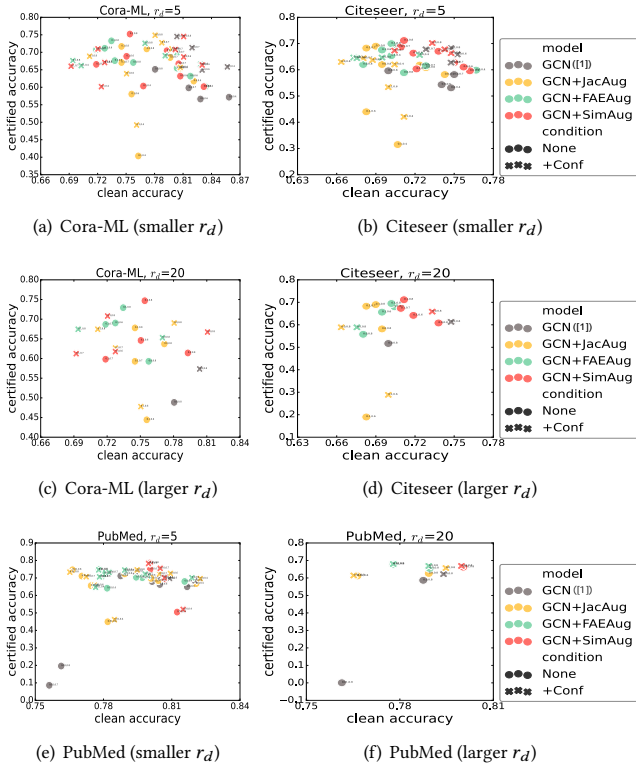


Figure 12: Clean accuracy and certified accuracy trade-off.

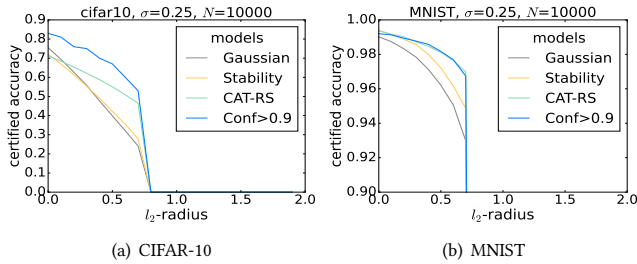


Figure 13: Applying AuditVotes (Confidence filter) to Gaussian [6] model for the image classification task.

Table 10: Certified accuracy comparison on MNIST.

$l_2$ -radius	0	0.3	0.5	0.7
Gaussian [6]	0.990	0.978	0.962	0.929
Stability [33]	<b>0.994</b>	0.985	0.972	0.948
CAT-RS [18]	0.993	0.987	0.981	<b>0.969</b>
Conf > 0.9 (Ours)	0.992	<b>0.988</b>	<b>0.982</b>	0.967

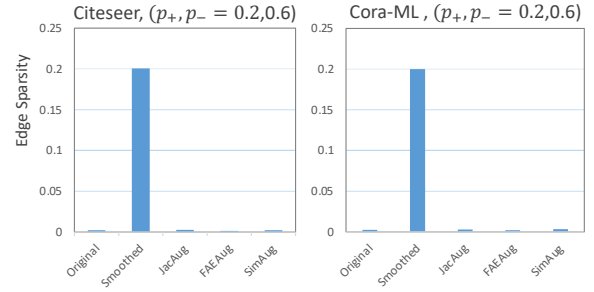


Figure 14: Edge sparsity of original graph, randomized graph with and without augmentations.

**Table 11: Empirical robust accuracy comparison among regular robust GNNs and smoothed GNNs. Attacker: IG-attack [51] (evasion setting), with 30 targeted nodes. (The attack encounters OOM on the PubMed dataset.)**

datasets	defense models	regular				smoothed ( $p_+ = 0.2, p_- = 0.3, N = 1000$ )			
	attack power	GCN	GAT	MedianGCN	AirGNN	GCN	<b>GCN+JacAug</b>	<b>GCN+FAEAug</b>	<b>GCN+SimAug</b>
Cora-ML	0	<u>0.989</u>	0.933	<b>1.000</b>	0.978	0.667	0.933	0.967	0.967
	1	0.922	0.856	0.900	<u>0.944</u>	0.667	0.933	<b>0.967</b>	<u>0.933</u>
	2	0.822	0.767	0.800	0.856	0.667	<u>0.933</u>	<b>0.967</b>	<u>0.933</u>
	3	0.756	0.700	0.589	0.744	0.667	<u>0.933</u>	<b>0.967</b>	<u>0.933</u>
	4	0.567	0.667	0.344	0.556	0.667	<u>0.933</u>	<b>0.967</b>	<u>0.933</u>
	5	0.400	0.444	0.244	0.467	0.667	<u>0.933</u>	<b>0.967</b>	<u>0.933</u>
Citeseer	0	0.789	0.789	0.722	<u>0.800</u>	0.167	<u>0.800</u>	0.733	<b>0.833</b>
	1	0.767	0.622	0.700	0.767	0.167	<u>0.800</u>	0.733	<b>0.833</b>
	2	0.489	0.456	0.378	0.522	0.167	<u>0.800</u>	0.733	<b>0.833</b>
	3	0.333	0.322	0.300	0.378	0.167	<u>0.800</u>	0.733	<b>0.833</b>
	4	0.333	0.289	0.189	0.333	0.167	<u>0.800</u>	0.733	<b>0.833</b>
	5	0.311	0.278	0.178	0.300	0.167	<u>0.800</u>	0.733	<b>0.833</b>